

DNA does not seem to cause any significant inflammation as demonstrated in our study (Figure 9). This may be because of the absence of cationic carrier, which normally enhance the inflammatory response.²⁵ Furthermore, skeletal muscle seems to internalize naked DNA more efficiently than other types of tissue.²⁶

Our study demonstrates that it is possible to achieve widespread gene expression in skeletal muscles by intravascular injection of naked DNA. Gene expression was detected in all muscle groups in either one or both hind limbs of mice (Figures 2–5 and 10, Table 1). There are apparently two major barriers for intravascular delivery of naked DNA to skeletal muscles. The first barrier is the endothelium wall, which apparently limits the extravasation of naked DNA to reach the muscle tissue. It was reported that the endothelium in muscle is different from the endothelium in liver or spleen. The latter is noncontinuous and fenestrated, containing many large pores. The former is of continuous and nonfenestrated type.²⁷ Despite its small size, naked DNA apparently cannot pass through the endothelium freely. In fact, the endothelium barrier is not only a barrier for naked DNA but also a barrier for viral vectors such as adenoviral and adeno-associated viral vectors as well.^{28,29} For gene therapy to be successful for systemic muscular disorders such as DMD, overcoming the endothelium barrier becomes the first prerequisite. Increasing the hydrodynamic pressure by injecting a large volume of DNA solution within a short time period seems to be an effective method to overcome this barrier. This method has been applied for both naked DNA- and viral vector-mediated gene transfer to muscles.^{11,28,29} A relatively large volume of solution in the vasculature may expand the endothelium and stretch the pores on the endothelium. Second, the elevated hydrodynamic pressure in the vasculature may force the DNA solution to pass through the endothelium and disperse it in the muscle tissue. Our results also showed a significant difference between intravenous injection and intra-artery injection. This significant difference may be simply due to the fact that arteries are less distensible than veins and so the plasmid solution is transmitted directly to the capillaries, where the hydrostatic pressure forces the solution into the interstitial space. In contrast, delivery via the venous system would lead to pooling of the plasmid solution in the veins as they can expand to accommodate very large volumes. In addition, major veins have valves that act to prevent blood flowing back towards the capillaries and these may have a barrier effect when venous delivery to the hind limbs is attempted. Other methods have also been used to enhance the extravasation of DNA. For example, Budker *et al*¹¹ have combined vasodilator and collagenase, which can digest the basal membrane of the endothelium, to increase the permeability of the endothelium and they observed further increase of gene expression. In our study, we have used histamine to increase the permeability of the endothelium. In histamine-treated mice, gene expression was enhanced about 10-fold in all muscle groups of the mouse legs. The application of histamine to increase the extravasation of adenoviral vector has also been tested and similar level of enhancement in gene expression was observed.²⁹ The combination of large volume injection with some agents that can increase the endothelium permeability seems to

be an effective method to overcome the endothelium barrier.

The second barrier for gene delivery to skeletal muscle appears to be the cellular uptake of naked DNA. Using fluorescence-labeled plasmid DNA, we clearly demonstrate that our method can deliver plasmid DNA to almost all muscle fibers in the tissue (Figure 8). However, only a relatively small percentage of muscle fibers showed gene expression when LacZ was used as a reporter gene. Therefore, muscle fibers seem to resist naked DNA uptake. This barrier appears to be the major barrier for gene delivery to skeletal muscle. Overcoming this barrier will have significant implication for gene therapy for DMD.

Compared to intramuscular injection, in which only a few percent of muscle fibers are been transfected, our method represents a significant advancement. Although in our LacZ study, the percentage of muscle fibers expressing LacZ is still low, the gene was expressed in all the muscle groups in mouse legs. Furthermore, it was reported that LacZ staining normally underestimates the gene expression about three-fold.³⁰ Indeed, our immunostaining with dystrophin gene expression revealed a much wider area of gene expression (Figure 10 and Table 1). However, it is not clear whether muscle function can be restored at this expression level. Function studies are required to assess the effect. Furthermore, data shown in Figure 10 seem to indicate that dystrophin was also expressed in the vasculature cells of the treated mouse. This could be due to the fact that the dystrophin gene used in this study was not controlled by a muscle-specific promoter. With the development of more efficient DNA vectors such as the ones with a targeting ligand attached,³¹ and with the use of a muscle-specific gene expression system, specific gene expression may be further increased.

In summary, the results of our study demonstrates the possibility of systemic delivery of naked DNA and achieve widespread expression of dystrophin gene in multiple skeletal muscles in *mdx* mice. However, the practical application of this method to treat DMD is still limited by the relatively low efficiency of DNA uptake by muscle cells and relatively short period of transgene expression. In addition, injecting large volume of solution locally may be applicable to human, as demonstrated by Zhang *et al*,¹² in monkeys. However, the application of this method to the diaphragm would be problematic. Different delivery method for the naked DNA to the diaphragm has recently been reported by this lab.³² It is possible to treat DMD by treating different organs separately. However, before this can happen, problems such as transfection efficiency and short-term expression have to be overcome.

Materials and methods

Plasmids

pCMV-Luc plasmid containing firefly luciferase cDNA driven by CMV immediate-early promoter was constructed by introducing the luciferase cDNA into pNGVL3 plasmid (National Gene Vector Laboratory, University of Michigan, MI, USA). pCMVLacZ plasmid was obtained from Invitrogen (Palo Alto, CA, USA). pFDPC plasmid containing full-length dystrophin cDNA

under the control of CMV promoter was constructed by digesting pSR α DMD (a gift from Dr Paula Clemens) with *NotI* and ligating to the *NotI* site of pcDNA 3 (Invitrogen, Palo Alto, CA, USA). For plasmid distribution study, pWIZ-Lux plasmid obtained from Gene Therapy System (GTS, San Diego, CA, USA) was labeled with rhodamine-labeled PNA according to a previous report.¹⁵ All plasmids were amplified in *Escherichia coli* and purified by Qiagen Giga plasmid preparation kit (Qiagen, Valencia, CA, USA).

Animal procedures

All experiments were performed using CD-1 mice (4–6 weeks old) or X-linked muscular dystrophy (*mdx*) mice (4–6 weeks old). Prior to any surgical procedure, the animals were anesthetized by intraperitoneal injection of 2,2,2-tribromoethanol (500 mg/kg). For plasmid injection, the tail artery or tail vein was cannulated with a 25 G butterfly needle connected to a polyethylene tubing (Harvard Apparatus, Holliston, MA, USA). The needle was subsequently fixed to the tail with instant adhesive (Loctite 404, Applied Industrial Technology, Pittsburgh, PA, USA). The abdomen was then opened to expose the aorta and the vena cava. Prior to injection, a microvascular clamp (Harvard Apparatus, Holliston, MA, USA) was placed on the aorta and vena cava at the location just below the kidneys (Figure 1) so that the DNA solution can pass through the common iliac artery and reach the leg muscles after injection from the tail artery or tail vein. In a typical experiment, 2 ml of PBS solution containing 100 μ g of luciferase plasmid or 400 μ g of β -galactosidase plasmid was injected in 5 s. Alternatively, DNA solution was injected to mice through the tail vein following clamping the aorta, vena cava and occlusion of the blood flow through one of the legs using modified artery forceps. The clamps were removed 15 s after injection and mice were allowed to recover from the effect of anesthesia. To examine the effect of histamine, 1 ml of PBS with or without histamine (10 mM) was first injected, and 5 min later, 2 ml of luciferase plasmid solution was then injected.

For the administration of dystrophin plasmid, the aorta of *mdx* mice was cannulated with a microcannula (Harvard Apparatus, Holliston, MA, USA), 1.5 ml of 10 mM histamine solution in PBS containing 500 μ g of the full-length dystrophin plasmid was injected in 5 s. After injection, the incision on aorta was closed with suture and mice were allowed to recover from the effect of anesthesia.

β -Galactosidase expression analysis

At 1 week after the intravascular injection of pCMVLacZ, mice were killed by cervical dislocation. All muscle groups were harvested and flash-frozen in isopentane cooled in liquid nitrogen. Serial cross-sections (12 μ m) were placed onto glass slides (Super-frost plus; Fisher Scientific, Pittsburgh, PA, USA) and kept at -80°C . X-gal staining was carried out using X-galactosidase staining kit (Invitrogen, Palo Alto, CA, USA) according to the manufacturer's procedure. Briefly, muscle sections were fixed in 1% glutaraldehyde for 10 min and then rinsed with PBS. Sections were then stained overnight for β -galactosidase activity by incubation at 37°C with 5-bromo-4-chloro-3-indolyl- β -D-galactopyranoside (X-gal, 1 mg/ml), 1 mM MgCl_2 , 5 mM potassium ferrocyanide, and

5 mM potassium ferricyanide in PBS. After washing in PBS, the slides were counterstained in alcoholic eosin and then dehydrated and mounted. Photographs were taken with a Nikon TE-300 fluorescence microscope. To quantitate the percentage of LacZ-positive fibers, the number of positive cells and the total number of cells were counted from 15 photographs covering different areas of muscle section.

Luciferase gene expression analysis

For luciferase assay, the entire muscle groups were collected from each mouse leg 2 days after injection, except for the time-course study. The muscles were homogenized in lysis buffer (1% Triton X-100, 2 mM EDTA, 0.1 M Tris, pH 7.8) using a tissue tearer (Biospec Products, Bartlesville, OK, USA). The homogenates were centrifuged at 14 000 g for 10 min at 4°C and 10 μ l of the supernatant was analyzed for luciferase activity using an LB 953 luminometer (Berthod). The results were expressed as relative light units per mg of tissue protein. Protein assay was carried out with the Coomassie plus reagent (Pierce, Rockford, IL, USA).

Plasmid distribution and histological examination of the muscle damage

PBS (2 ml) solution containing 100 μ g of luciferase plasmid labeled with rhodamine-PNA was injected through the tail artery as described above. At 5 and 30 min after injection, the quadriceps were collected, flash-frozen and sectioned. The slides were examined and photographed using a Nikon T-300 fluorescence microscope. For the muscle damage study, 2 ml of PBS solution containing luciferase plasmid was injected as above. Quadriceps were collected at 2 and 7 days after injection, sectioned and stained with H&E.

Immunofluorescence detection of dystrophin gene expression

Serial crosscryosections (6 μ m) were collected. Immunostaining of dystrophin was performed with the Mouse-on-Mouse Kit (Vector Laboratories) according to the manufacturer's protocol without fixing the muscle sections. Primary monoclonal antibody against the C-terminus of dystrophin (NCL-Dys2; 1:20 dilution) was purchased from NovoCastra Laboratories (Burlingame, CA, USA). Muscle cell nuclei were counterstained with a mounting medium containing 4', 6'-diamidino-2-phenylindole (DAPI) (Vector Laboratories). For quantitation of dystrophin-positive fibers, the number of dystrophin-positive cells and the total number of cells were counted from 15 photographs covering different areas of muscle section. For intravenously injected animals, the sections were preincubated for 1 h at room temperature with 10% horse serum in PBS (pH 7.4) and then incubated overnight with affinity purified rabbit polyclonal anti-dystrophin antibody 6–10 (a gift from EP Hoffman).^{33,34} After four rinses in 10% horse serum/PBS, the sections were incubated with Alexa Fluor 568 goat anti-rabbit antibody (Molecular Probes, 1:200 dilution) for 1 h. As controls, the muscle sections from C57BL/10 and untreated *mdx* mice were similarly processed. The sections were examined and photographed with a Nikon TE-300 fluorescence microscope.

Dystrophin assay by Western blot

Methods. Mice quadriceps were sectioned and extracted at TEE buffer that contains 20 mM Tris pH 8.0, 1 mM EDTA, 1 mM EGTA and then mixed with same volume of 10% SDS and incubate in ice for 30 min. Protein concentration was determined using BCA protein assay kit (Biorad). The samples were then subjected to electrophoresis of 7.5% SDS-PAGE gel, transferred to nitrocellulose membrane. Dystrophin expression was then detected using a high-affinity antidystrophin antibody anti 6-10, a generous gift from Dr LM Kunkel (Children's hospital and Harvard Medical School, Boston, MA, USA), and visualized with anti-rabbit secondary antibody linked to horseradish peroxidase and chemiluminescence (Amersham).

Acknowledgements

This work was supported in part by Muscular Dystrophy Association grant and NIH grant PO1 AR45925 (L. Huang) and grant from the Uehara memorial Foundation (M. Nishikawa). We thank Dr Paula Clemens for providing the dystrophin plasmid and *mdx* mice. Kenneth W Liang and Makiya Nishikawa were post-doctoral fellows of Duchenne Muscular Dystrophy Research Center, University of Pittsburgh.

References

- Hoffman EP, Brown Jr RH, Kunkel LM. Dystrophin: the protein product of the Duchenne muscular dystrophy locus. *Cell* 1987; 51: 919-928.
- Zubrzycka-Gaarn EE et al. The Duchenne muscular dystrophy gene product is localized in sarcolemma of human skeletal muscle. *Nature* 1988; 333: 466-469.
- Campbell KP, Kahl SD. Association of dystrophin and an integral membrane glycoprotein. *Nature* 1989; 338: 259-262.
- Acsadi G et al. Human dystrophin expression in *mdx* mice after intramuscular injection of DNA constructs [see comments]. *Nature* 1991; 352: 815-818.
- Deconinck N et al. Functional protection of dystrophic mouse (*mdx*) muscles after adenovirus-mediated transfer of a dystrophin minigene. *Proc Natl Acad Sci USA* 1996; 93: 3570-3574.
- Yang L et al. Adenovirus-mediated dystrophin minigene transfer improves muscle strength in adult dystrophic (MDX) mice. *Gene Therapy* 1998; 5: 369-379.
- Gilbert R et al. Prolonged dystrophin expression and functional correction of *mdx* mouse muscle following gene transfer with a helper-dependent (guttled) adenovirus-encoding murine dystrophin. *Hum Mol Genet* 2003; 12: 1287-1299.
- Harper SQ et al. Modular flexibility of dystrophin: implications for gene therapy of Duchenne muscular dystrophy. *Nat Med* 2002; 8: 253-261.
- Watchko J et al. Adeno-associated virus vector-mediated mini-dystrophin gene therapy improves dystrophic muscle contractile function in *mdx* mice. *Hum Gene Ther* 2002; 13: 1451-1460.
- Mumper RJ et al. Protective interactive noncondensing (PINC) polymers for enhanced plasmid distribution and expression in rat skeletal muscle. *J Control Rel* 1998; 52: 191-203.
- Budker V et al. The efficient expression of intravascularly delivered DNA in rat muscle. *Gene Therapy* 1998; 5: 272-276.
- Zhang G et al. Efficient expression of naked DNA delivered intraarterially to limb muscles of nonhuman primates. *Hum Gene Ther* 2001; 12: 427-438.
- Levy MY et al. Characterization of plasmid DNA transfer into mouse skeletal muscle: evaluation of uptake mechanism, expression and secretion of gene products into blood. *Gene Therapy* 1996; 3: 201-211.
- Wolff JA et al. Long-term persistence of plasmid DNA and foreign gene expression in mouse muscle. *Hum Mol Genet* 1992; 1: 363-369.
- Zelphati O et al. Gene chemistry: functionally and conformationally intact fluorescent plasmid DNA. *Hum Gene Ther* 1999; 10: 15-24.
- Karpati G et al. Dystrophin is expressed in *mdx* skeletal muscle fibers after normal myoblast implantation. *Am J Pathol* 1989; 135: 27-32.
- Akkaraju GR et al. Herpes simplex virus vector-mediated dystrophin gene transfer and expression in MDX mouse skeletal muscle. *J Gene Med* 1999; 1: 280-289.
- Acsadi G et al. Dystrophin expression in muscles of *mdx* mice after adenovirus-mediated *in vivo* gene transfer. *Hum Gene Ther* 1996; 7: 129-140.
- Jani A et al. Generation, validation, and large scale production of adenoviral recombinants with large size inserts such as a 63 kb human dystrophin cDNA. *J Virol Methods* 1997; 64: 111-124.
- Wang B, Li J, Xiao X. Adeno-associated virus vector carrying human minidystrophin genes effectively ameliorates muscular dystrophy in *mdx* mouse model. *Proc Natl Acad Sci USA* 2000; 97: 13714-13719.
- Yanagihara I et al. Expression of full-length human dystrophin cDNA in *mdx* mouse muscle by HVJ-liposome injection. *Gene Therapy* 1996; 3: 549-553.
- Feero WG et al. Viral gene delivery to skeletal muscle: insights on maturation-dependent loss of fiber infectivity for adenovirus and herpes simplex type 1 viral vectors. *Hum Gene Ther* 1997; 8: 371-380.
- Krieg AM et al. CpG motifs in bacterial DNA trigger direct B-cell activation. *Nature* 1995; 374: 546-549.
- McMahon JM et al. Inflammatory responses following direct injection of plasmid DNA into skeletal muscle. *Gene Therapy* 1998; 5: 1283-1290.
- Whitmore M, Li S, Huang L. LPD lipopolyplex initiates a potent cytokine response and inhibits tumor growth. *Gene Therapy* 1999; 6: 1867-1875.
- Davis HL et al. Plasmid DNA is superior to viral vectors for direct gene transfer into adult mouse skeletal muscle. *Hum Gene Ther* 1993; 4: 733-740.
- Taylor A, Granger D. The cardiovascular system: microcirculation. In: Renkin E, Michel CC, Geiger SR (eds). *Handbook of Physiology*, Am. Physiol. Soc.: Bethesda, MD 1984: 467-520.
- Cho WK et al. Modulation of Starling forces and muscle fiber maturity permits adenovirus-mediated gene transfer to adult dystrophic (*mdx*) mice by the intravascular route. *Hum Gene Ther* 2000; 11: 701-714.
- Greelish JP et al. Stable restoration of the sarcoglycan complex in dystrophic muscle perfused with histamine and a recombinant adeno-associated viral vector. *Nat Med* 1999; 5: 439-443.
- Couffignal T et al. Histochemical staining following LacZ gene transfer underestimates transfection efficiency. *Hum Gene Ther* 1997; 8: 929-934.
- Liang KW, Hoffman EP, Huang L. Targeted delivery of plasmid DNA to myogenic cells via transferrin-conjugated peptide nucleic acid. *Mol Ther* 2000; 1: 236-243.
- Liu F et al. Transfer of full-length Dmd to the diaphragm muscle of Dmd(*mdx/mdx*) mice through systemic administration of plasmid DNA. *Mol Ther* 2001; 4: 45-51.
- Koenig M, Kunkel LM. Detailed analysis of the repeated domain of dystrophin reveals 4 potential hinge regions that may confer flexibility. *J Biol Chem* 1990; 265: 4560-4566.
- Hoffman EP et al. Somatic reversion/suppression of the mouse *mdx* phenotype *in vivo*. *J Neurol Sci* 1990; 99: 9-25.

Restricted cytokine production from mouse peritoneal macrophages in culture in spite of extensive uptake of plasmid DNA

KEI YASUDA, HIROKI KAWANO, IKUKO YAMANE, YOSHIYUKI OGAWA, TAKAHARU YOSHINAGA, MAKIYA NISHIKAWA & YOSHINOBU TAKAKURA *Department of Biopharmaceutics and Drug Metabolism, Graduate School of Pharmaceutical Sciences, Kyoto University, Sakyo-ku, Kyoto, Japan*

SUMMARY

The production of inflammatory cytokines from macrophages (M ϕ), upon stimulation with plasmid DNA (pDNA) containing CpG motifs, is a critical process for DNA-based therapies such as DNA vaccination and gene therapy. We compared M ϕ activation, following stimulation with naked pDNA, based on the production of cytokines from cell lines (RAW264.7 and J774A1) and peritoneal M ϕ s in primary culture. The M ϕ cell lines RAW264.7 and J774A1 produced a significant amount of tumour necrosis factor- α (TNF- α) upon stimulation with naked pDNA and this response required endosomal acidification. On the other hand, peritoneal M ϕ s (both resident and elicited) in primary culture did not secrete TNF- α or interleukin-6, although they contain the mRNA of toll-like receptor-9 (TLR-9) and are able to respond to CpG oligodeoxynucleotides. This unresponsiveness was not a result of impaired cellular uptake of pDNA because the primary cultured M ϕ s showed a higher uptake of pDNA than the RAW264.7 and J774A1 cell lines. These findings have important implications for M ϕ activation by naked pDNA as it has been generally assumed that pDNA that contains CpG motifs is a potent agent for inducing inflammatory cytokines *in vivo*, based on evidence from *in vitro* studies using M ϕ cell lines.

INTRODUCTION

Bacterial DNA and plasmid DNA (pDNA) contain a relatively high frequency of unmethylated CpG dinucleotides (CpG motifs), which are suppressed and methylated in vertebrate DNA. The immune system has evolved a defence mechanism based on the recognition of these CpG motifs.^{1,2} For example, bacterial DNA and CpG oligodeoxynucleotides (ODN) can activate cells of the innate immune system, such as macrophages (M ϕ s) and dendritic cells (DCs), to secrete pro-inflammatory cytokines, including tumour necrosis factor- α (TNF- α), interleukin (IL)-1, IL-6 and IL-12.^{3–7} This phenomenon appears

to be advantageous as far as DNA vaccination is concerned⁸ because it is crucial in the subsequent development of T-helper 1 (Th1)-biased T-cell lineages in response to CpG DNA.^{9–11} On the other hand, recent reports have demonstrated that these inflammatory cytokines inhibit transgene expression with pDNA.^{12,13} Therefore, cytokine production from M ϕ s upon stimulation with pDNA containing CpG motifs is a critical process in the application of DNA-based therapies, such as DNA vaccination and gene therapy.

Recently it was reported that Toll-like receptor-9 (TLR-9), expressed in M ϕ s and DCs, recognizes the CpG motifs.^{14,15} As a first cytosolic event, the adaptor molecule MyD88 is recruited to the receptor complex, followed by engagement of IL-1 receptor-associated kinase (IRAK) and the adapter molecule, TRAF6.¹⁶ Oligomerization of TRAF6 leads to the activation of downstream kinases, such as the stress kinase JNK1/2 and the I κ B kinase (IKK) complex.¹⁷ This, in turn, results in activation of transcription factors such as AP-1 and nuclear factor (NF)- κ B. Proof of these phenomena has been obtained using synthetic phosphorothioate CpG ODN (S-ODN), small single-stranded DNA. It is generally assumed that the same mechanism would be involved in cellular activation by pDNA because its backbone contains similar immunostimulatory sequences. In fact, a variety of studies have demonstrated that CpG motifs are required to stimulate immune responses following DNA vaccination.

Received 28 October 2003; revised 4 December 2003; accepted 9 December 2003.

Abbreviations: DC, dendritic cell; FBS, fetal bovine serum; IL, interleukin; LPS, lipopolysaccharide; M ϕ , macrophage; ODN, oligodeoxynucleotides; pDNA, plasmid DNA; TCA, trichloroacetic acid; TLR, toll-like receptor; TNF- α , tumour necrosis factor- α .

Correspondence: Yoshinobu Takakura, Department of Biopharmaceutics and Drug Metabolism, Graduate School of Pharmaceutical Sciences, Kyoto University, 46-29, Yoshidashimoadachi-cho, Sakyo-ku, Kyoto 606-8501, Japan. E-mail: takakura@pharm.kyoto-u.ac.jp

Although there is a growing body of information reporting M ϕ activation by CpG DNA, most studies have been performed using M ϕ cell lines derived from the mouse. Few studies have been reported using primary cultured M ϕ s freshly isolated from animals, which would be a better model than immortalized cells lines as far as reflecting the *in vivo* situation is concerned.

Previously we have demonstrated that Kupffer cells (liver-resident M ϕ s) play an important role in the processing of pDNA after intravenous injection into mice.¹⁸ *In vitro* experiments, using mouse peritoneal resident M ϕ s, have also shown that primary cultured M ϕ s take up pDNA efficiently via a scavenger receptor-like mechanism and in a specific manner.^{19,20} In the present study, we evaluated M ϕ activation, following stimulation with naked pDNA, using mouse peritoneal resident and elicited cultured M ϕ s in comparison with the M ϕ cell lines RAW264.7 and J774A1. We found that the peritoneal M ϕ s showed very low or almost no secretion of inflammatory cytokines following stimulation with pDNA, in spite of extensive uptake of CpG DNA. These results contrast with our recent finding that peritoneal M ϕ s and RAW264.7 cells show similar responsiveness to pDNA complexed with cationic liposomes.²¹

MATERIALS AND METHODS

Chemicals

RPMI-1640, Dulbecco's modified Eagle's minimal essential medium (DMEM), Hanks' balanced salt solution (HBSS) and thioglycolate broth were obtained from Nissui Pharmaceutical (Tokyo, Japan). Triton X-114 was purchased from Nacal Tesque (Kyoto, Japan).

Cell cultures

Male ICR mice (5 weeks of age) were purchased from the Shizuoka Agricultural Cooperative Association for Laboratory Animals (Shizuoka, Japan). Resident M ϕ s were collected (in RPMI-1640) from the peritoneal cavity of unstimulated mice. Cells were washed, suspended in RPMI-1640 supplemented with 10% fetal bovine serum (FBS), penicillin G (100 U/ml), streptomycin (100 μ g/ml) and amphotericin B (1.2 μ g/ml), and then plated on 24-well culture plates (Falcon; Becton Dickinson, Lincoln Park, NJ), at a density of 5×10^5 cells/well, for the cellular association experiments and activation experiments. For confocal microscopic observations, peritoneal cells were plated on a cover glass, in a 12-well culture plate, at a density of 5×10^5 cells/well. After a 2-hr incubation at 37° in 5% CO₂/95% air, adherent M ϕ s were washed three times with RPMI-1640 to remove non-adherent cells and then cultured under the same conditions for 24 hr. For elicited M ϕ s, all the processes were the same, except that 1 ml of 2.9% thioglycolate broth was injected intraperitoneally into mice 4 days prior to the collection of M ϕ s. RAW264.7 or J774A1 cells were cultured in RPMI-1640 supplemented with 10% FBS, penicillin G (100 U/ml) and streptomycin (100 μ g/ml). They were then plated on a 24-well culture plate at a density of 2.5×10^5 cells/ml and cultured for 24 hr.

Plasmid DNA

The vector pCDNA3 was purchased from Invitrogen (Carlsbad, CA). The vector pCMV-Luc, encoding the firefly luciferase gene, was constructed as described previously.²² pCDNA3

contains 26 5'-Pur-Pur-CpG-Pyr-Pry-3' sequences, including two GACGTT sequences which have been reported to be the most potent sequences for mice.⁷ For the cellular-association experiment, pCMV-Luc was radiolabelled with [α -³²P]dCTP by nick translation.²³ The reaction was performed on 1 μ g of pDNA (pCMV-Luc) in a final volume of 40 μ l. The incubation buffer was 50 mM Tris-HCl, pH 7.8, 10 mM MgCl₂, 0.1 mM dithiothreitol (DTT) and 0.0025% bovine serum albumin (BSA). The reaction was initiated by adding 4 U of *Escherichia coli* (E. coli) DNA Polymerase I (Takara, Kyoto, Japan) and 0.0004 U of DNase I (Takara) in the presence of 40 nM unlabelled triphosphate (dATP, dGTP, dTTP) and [α -³²P]dCTP (3.7 MBq, 100 μ Ci). After a 2-hr incubation at 15°, the reaction was terminated by heating at 70° for 10 min. Unincorporated nucleotides were removed using a Sephadex G-50 column. For the confocal microscopy study, pCMV-Luc was labelled using a Fasttag Texas Red labelling kit, according to the manufacturer's instructions (Vector Laboratories, Burlingame, CA).

Purification of pDNA

To minimize any activation as a result of contaminating lipopolysaccharide (LPS), we used DNA samples extensively purified with Triton X-114, a non-ionic detergent. Extraction of endotoxin from pDNA, methylated-CpG pDNA, E. coli DNA and calf thymus DNA samples was performed according to previously published methods,^{24,25} with slight modifications. DNA samples were purified by extraction with phenol-chloroform-isoamyl alcohol (25 : 24 : 1; v/v/v) and ethanol precipitation. Ten micrograms of DNA was diluted with 20 ml of pyrogen-free water, then 200 μ l of Triton X-114 was added, followed by mixing. The solution was placed on ice for 15 min and then incubated for 15 min at 55°. Subsequently, the solution was centrifuged (20 min, 25°, 600 g). The upper phase was transferred to a new tube, 200 μ l of Triton X-114 was added and the previous steps were repeated three or more times. The activity of LPS was measured by the Limulus amoebocyte lysate (LAL) assay using the Limulus F Single Test kit (Wako, Tokyo, Japan). After purification using the Endo-free™ plasmid Giga kit, 1 μ g/ml pDNA was found to contain 0.01–0.05 endotoxin units (EU)/ml. After extraction using Triton X-114, the endotoxin levels of DNA samples could no longer be determined by the LAL assay, i.e. 1 μ g/ml DNA contained less than 0.001 EU/ml. Without extraction of endotoxin by Triton X-114, 100 μ g/ml naked pDNA, containing 1–5 EU/ml, was able to stimulate the release of 521 ± 73 pg/ml TNF- α at 24 hr.

ODN

Phosphorothioate ODN was purchased from GENSET (Paris, France). The sequence of CpG S-ODN 1668 (a proven activator of murine immune cells, as previously described) is 5'-TCCAT-GACGTTCCCTGATGCT-3'.^{5,26} Phosphorothioate non-CpG ODN 1720 (5'-TCCATGAGCTTCCCTGATGCT-3') was used as a control. CG motifs and control GC sequences are underlined. Fluorescein isothiocyanate (FITC)-labelled CpG ODN was purchased from Sawady Technology (Tokyo, Japan).

Reverse transcription-polymerase chain reaction (RT-PCR)

Total RNA was extracted from cells using TRIzol (Invitrogen). Five micrograms of RNA was reverse-transcribed to complementary

DNA using the SUPERScript First-Strand Synthesis System for RT-PCR (Invitrogen). Fragments were amplified with *Taq* polymerase (Takara) using the following primer pairs: mTLR-9, 5'-CCGCAAGACTCTATTTGTGCTGG-3' and 5'-TGTCCTAGTCAGGGCTGTAAGCAG-3',¹⁵ and glyceraldehyde-3-phosphate dehydrogenase (GAPDH), 5'-TC-ACCATCTCCAGGAGCGA-3' and 5'-ACCAGGAAATGAGCTTGACA-3'. The PCR temperature and cycles were as follows: 60 seconds at 95°, 90 seconds at 56° and 30 seconds at 72°, for 30 cycles. The size of the mTLR-9 and GAPDH products were 260 bp and 720 bp, respectively.

For the fragmentation or denaturation of DNA, pDNA were diluted in endotoxin-free water, to a concentration of 1 mg/ml in a 0.5 ml tube, and sonicated for 2 hr in an ultrasonic automatic washer (Iuchi, Tokyo, Japan). Separately, DNA was heat-denatured at 95° for 10 min. DNA was incubated at 4° before use.

Cytokine secretion

Mouse Mφs, resident and elicited peritoneal Mφs from ICR mice, and the Mφ cell lines, RAW264.7 and J774A1, were washed three times with 0.5 ml of RPMI-1640 before use. Naked DNA was diluted in 0.5 ml of Opti-MEM and the cells were incubated for 8 hr with this solution. Then, the cells were washed with RPMI-1640 and incubated with RPMI-1640 containing 10% FBS, continuously, for specified time-periods of up to 48 hr. In the inhibition experiments, cells were incubated with the medium containing an inhibitor alone, at various concentrations, for 30 min, then incubated with the medium containing DNA or liposome formulations together with the inhibitor. At the indicated time-points, the supernatants were collected for enzyme-linked immunosorbent assay (ELISA) and stored at -80°. The levels of TNF-α and IL-6 in the supernatants were determined by using the OptEIA™ set (Pharmin-gen, San Diego, CA). The detection limit of these sets was 15.6 pg/ml for both cytokines.

Cellular-association experiments

Mouse peritoneal Mφs and RAW264.7 cells were cultured in 24-well plates. The cells were washed twice with HBSS (without phenol red) and then incubated, at 37°, with HBSS containing trypsin (50 µg/ml). Then, the cells were washed with HBSS and incubated with HBSS containing ³²P-labelled pDNA (0.1 µg/ml). After a 3-hr incubation at 4°, the cells were washed three times with ice-cold HBSS and then solubilized with 1.0 ml of 0.3 N NaOH containing 0.1% Triton-X-100. Aliquots were taken for the determination of ³²P radioactivity using an LSA-500 scintillation counter (Beckman, Tokyo, Japan). The protein content was measured using the modified Lowry method²⁷ with BSA as a standard.

Trichloroacetic acid (TCA) precipitation experiments

After the cellular-association experiments, the medium and cell lysate containing radioactivity derived from ³²P-labelled pDNA were subjected to TCA-precipitation experiments to assess the degradation of pDNA by Mφs. A portion of the cell lysate was directly subjected to radioactivity counting and the protein content was measured as described above. The cell lysis solution was neutralized with 1 N HCl, and the same volume of

10 mM Tris-HCl, 1 mM EDTA (TE)-saturated phenol (pH 7.8) was added. The mixture was vortexed and centrifuged at 13 500 g for 10 min. The upper phase was transferred to another tube to which the same volume of ice-cold 10% TCA was added, and the tube was vortexed. After a 10-min incubation on ice, the solution was centrifuged at 13 500 g for 25 min. Supernatants were used for the determination of radioactivity. To quantify the amount of free [α-³²P]dCTP in ³²P-labelled pDNA, TCA precipitation of a standard sample was performed.

Confocal microscopy

Cells were washed three times with 1.0 ml of HBSS and then incubated, in HBSS, at 4° for 10 min. The cells were then incubated with HBSS containing Texas Red-labelled pDNA and FITC-labelled CpG S-ODN at 4° for 30 min. The cells were washed five times with HBSS and incubated at 37° for 15 min. Then, the cells were fixed with 4% paraformaldehyde for 10 min. The cells were scanned by confocal microscopy (MRC-1024; Bio-Rad, Hercules, CA).

RESULTS

Peritoneal Mφs do not secrete inflammatory cytokines upon stimulation with naked pDNA

Secretion of inflammatory cytokines, induced by CpG DNA, was examined using mouse Mφ cell lines and peritoneal Mφs. *E. coli* DNA and pDNA were models of CpG DNA, and calf thymus DNA was used as non-CpG DNA. DNA was extensively purified with phenol and Triton X-114 to avoid contamination with LPS and some bacterial proteins. Two different cell lines – RAW264.7 and J774A1 – secreted a large amount of TNF-α, upon stimulation with naked *E. coli* DNA and pDNA, in a concentration-dependent manner (Fig. 1). Calf thymus DNA was unable to induce the secretion of TNF-α. Digested *E. coli* DNA was unable to stimulate the secretion of TNF-α from RAW264.7 cells. These results indicated that, similarly to ODN, naked DNA also activates these Mφ cell lines to produce inflammatory cytokines in a CpG motif-dependent manner. Similar experiments were carried out using two types of mouse peritoneal Mφs – resident and elicited Mφs – isolated from male ICR mice. Surprisingly, CpG DNA, pDNA and *E. coli* DNA were unable to induce TNF-α release from either resident or elicited Mφs in primary culture, even at a high concentration (100 µg/ml DNA) for up to 24 hr (Fig. 2). Another inflammatory cytokine, IL-6, also failed to be detected in resident Mφs. LPS stimulated all types of Mφs to secrete TNF-α.

Expression of TLR-9 mRNA and cytokine release induced by CpG DNA from peritoneal Mφs and RAW264.7 cells

TLR-9 recognizes bacterial CpG motifs. To confirm the reactivity of peritoneal Mφs with CpG DNA, we tested the mRNA expression of TLR-9 in these cells by RT-PCR. Both resident peritoneal Mφs and RAW264.7 cells showed TLR-9 mRNA expression (Fig. 3). Moreover, CpG ODN 1668 was able to induce TNF-α from the resident Mφs (Fig. 4a). CpG DNA requires endocytosis and endosomal acidification to induce inflammatory responses.^{26,28,29} It was shown that endosomal

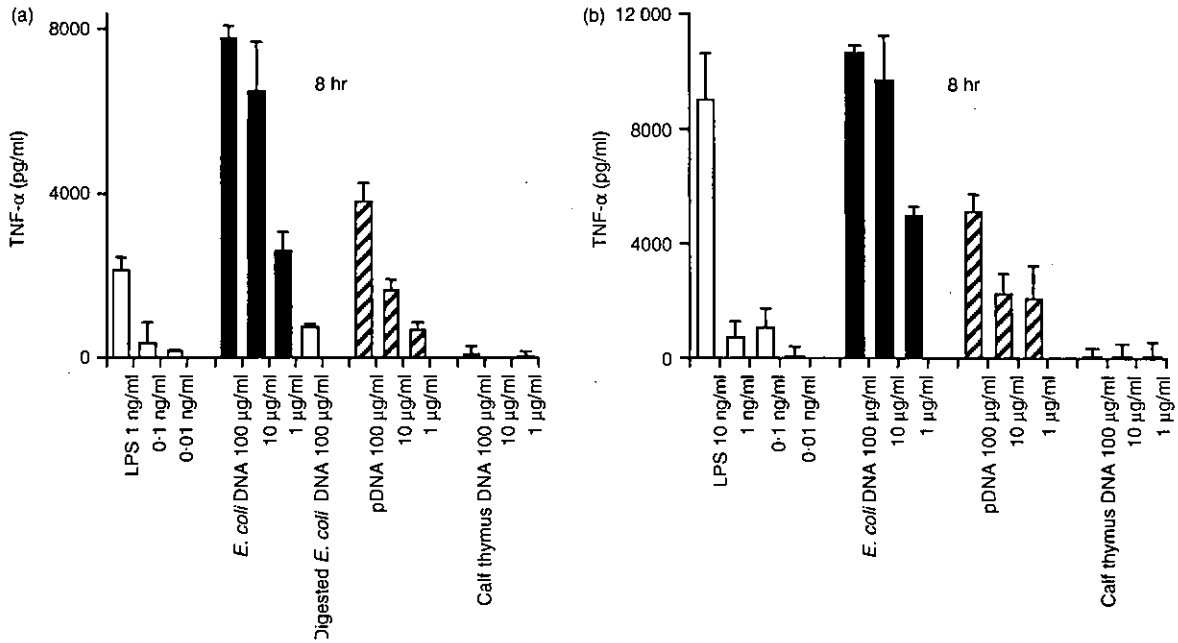


Figure 1. Cytokine release induced by naked plasmid DNA (pDNA) or other DNAs from macrophage (M ϕ) cell lines. RAW264.7 cells (a) or J774A1 cells (b) were incubated with lipopolysaccharide (LPS) (white bar), *Escherichia coli* (*E. coli*) DNA (black bar), pDNA (hatched bar), or calf thymus DNA (shaded bar) for 8 or 24 hr. The amount of cytokines released from the M ϕ s was quantified by enzyme-linked immunosorbent assay (ELISA). The concentration of cytokines present in medium only was subtracted from the cytokine concentration in each sample. Each result represents the mean and standard deviation ($n = 3$).

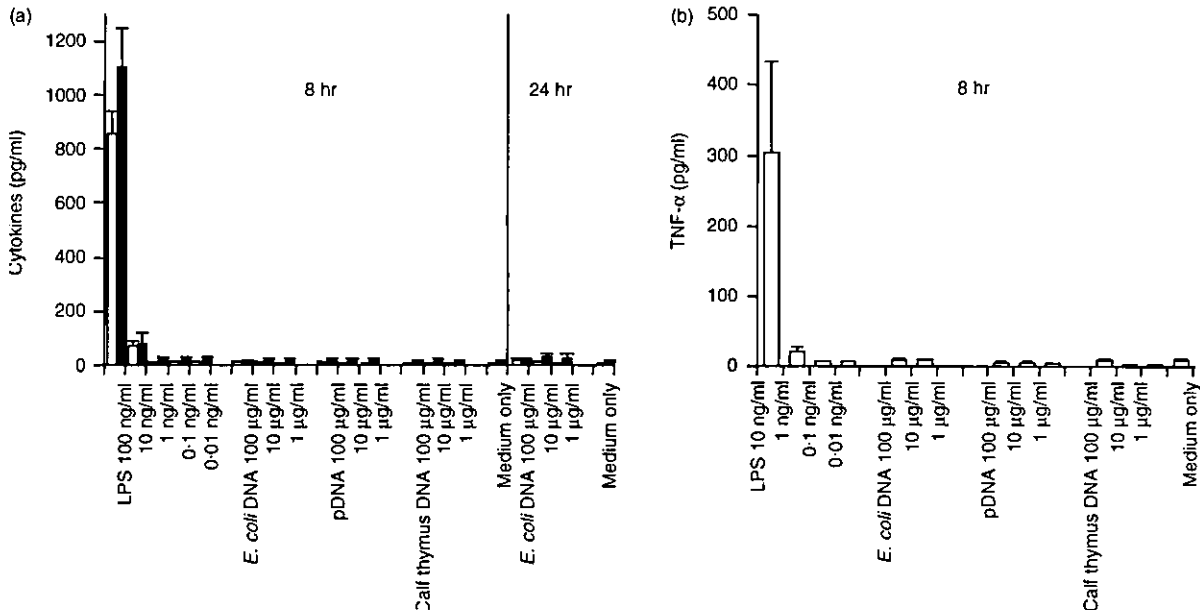


Figure 2. Cytokine release induced by naked plasmid DNA (pDNA) or other DNAs from primary cultured macrophages (M ϕ s). Resident M ϕ s (a) or elicited M ϕ s (b) were incubated with lipopolysaccharide (LPS), *Escherichia coli* (*E. coli*) DNA, pDNA, or calf thymus DNA for 8 or 24 hr. The amount of tumour necrosis factor- α (TNF- α) (white bars) and interleukin-6 (IL-6) (black bars) released from the M ϕ s was quantified by enzyme-linked immunosorbent assay (ELISA). Each result represents the mean and standard deviation ($n = 3$).

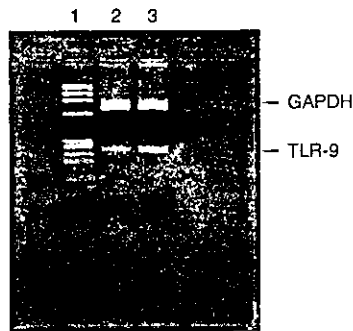


Figure 3. Expression of Toll-like receptor-9 (TLR-9) mRNA in macrophages (M ϕ s). Total RNA was extracted from resident M ϕ s or RAW264.7 cells. mRNA expression of TLR-9 was determined by reverse transcription-polymerase chain reaction (RT-PCR). DNA mobility was analysed by agarose-gel electrophoresis (3–5% gel). Lane 1, Φ -HaeIII marker; lane 2, resident M ϕ s; lane 3, RAW264.7 cells. GAPDH, glyceraldehyde-3-phosphate dehydrogenase.

acidification inhibitors, such as bafilomycin A, chloroquine or monensin, inhibited cytokine secretion by CpG ODN from RAW264.7 cells.²⁸ Therefore, the effect of these inhibitors on cytokine release from resident M ϕ s was examined. The endocytosis inhibitor, cytochalasin B, inhibited the induction of TNF- α by CpG ODN from the resident M ϕ s. TNF- α secretion was also significantly reduced by these endosomal acidification inhibitors.

In contrast to primary cultured M ϕ s, RAW264.7 cells and J774A1 cells could be stimulated by pDNA to produce TNF- α (Fig. 1). The effect of inhibitors of endocytosis or endosomal acidification on the cytokine responses induced in RAW264.7 cells was examined. Cytochalasin B inhibited the TNF- α

release that was stimulated by pDNA. Monensin, bafilomycin A and chloroquine, inhibitors of endosomal acidification, suppressed the induction of TNF- α (Fig. 4), suggesting that similar mechanisms are involved in cytokine induction by pDNA in M ϕ s.

Cellular uptake and subsequent degradation of pDNA are not major factors in the unresponsiveness of peritoneal M ϕ s to pDNA

It has been reported that TLR-9 is an intracellular protein.³⁰ To determine whether the difference in activation induced by CpG DNA (other than CpG S-ODN) is the result of a difference in the cellular uptake of DNA, we compared the degree of binding and uptake of ³²P-labelled pDNA in all the M ϕ types used in this study. The cellular association of ³²P-labelled pDNA in the RAW264.7 and J774A1 cells was time- and temperature-dependent (Fig. 5). The resident and elicited M ϕ s showed a significantly higher cellular association of ³²P-labelled pDNA at both 4° and 37° than observed in the RAW264.7 and J774A1 cell lines. In the confocal microscopy study, fluorescein-labelled pDNA was also taken up by both RAW264.7 cells and resident M ϕ s. The latter took up pDNA more efficiently (Fig. 5).

After endocytosis, DNA is degraded by deoxyribonuclease II (DNase II) in the lysosomal compartment³¹ and this event may affect the recognition of CpG motifs by TLR-9 in M ϕ s. Therefore, the difference in degradation efficiency may account for the distinct responsiveness between primary M ϕ s and cell lines. To explore the effect of degradation of pDNA on immunoinactivation, we measured the amount of ³²P-labelled pDNA degraded by RAW264.7 cells and resident M ϕ s by the TCA precipitation method. The TCA-soluble degradation products will be small DNA fragments (short oligodeoxynucleotides), as

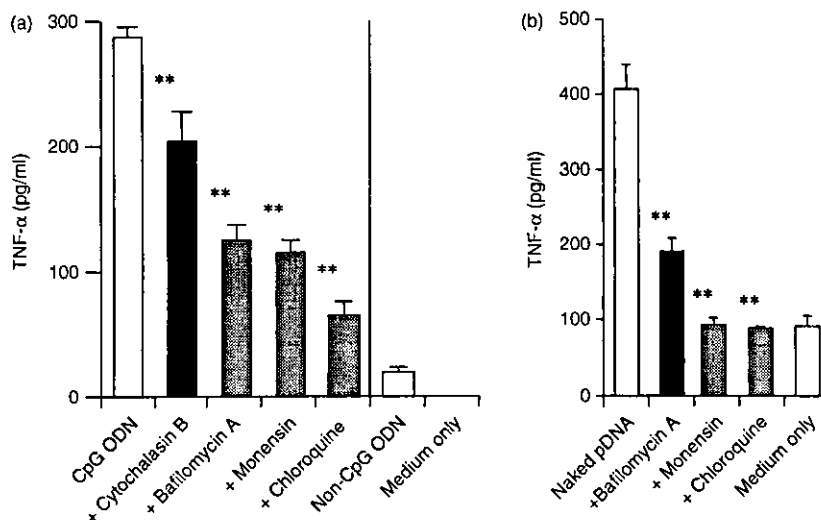


Figure 4. Tumour necrosis factor- α (TNF- α) release induced by CpG oligodeoxynucleotides (ODN) or non-CpG ODN from resident macrophages (M ϕ s) (a) or plasmid DNA (pDNA) from RAW264.7 cells (b). (a) Resident M ϕ s were incubated with 10 μ M CpG ODN or non-CpG ODN, in the presence or absence of inhibitors, at 37° for 8 hr. (b) RAW264.7 cells were incubated with 10 μ g/ml CpG pDNA, in the presence or absence of inhibitors, at 37° for 2 hr. Each result represents the mean and standard deviation ($n = 3$). Differences in the cytokine levels of the samples treated with CpG ODN only and CpG ODN + inhibitors (bafilomycin A, cytochalasin B, chloroquine and monensin) were analysed statistically by using the Student's *t*-test. ** $P < 0.01$.

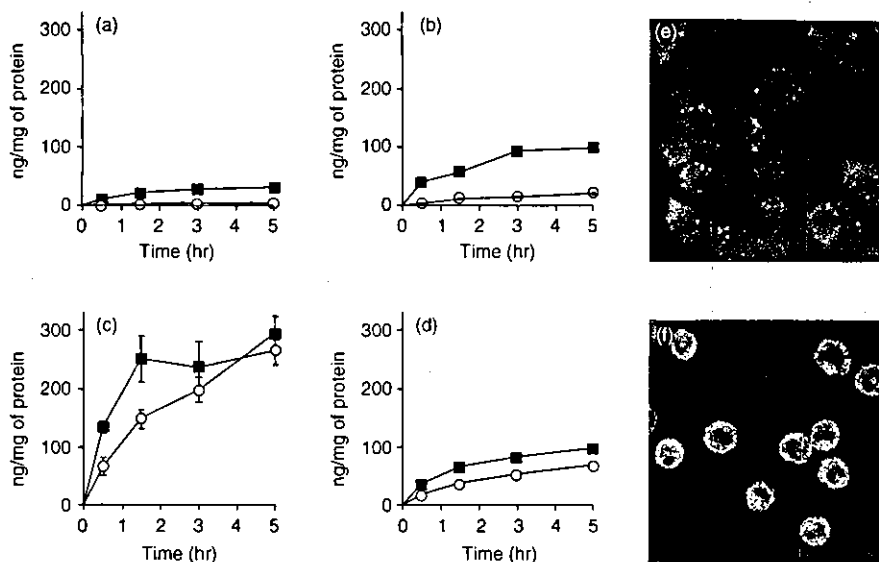


Figure 5. Cellular association time-course experiments of ³²P-labelled plasmid DNA (pDNA) in RAW264.7 cells (a), J774A1 cells (b), and resident (c) or elicited (d) macrophages (Mφs); and cellular localization of pDNA in RAW264.7 cells (e) or resident Mφs (f). (a–d) Cells were incubated with ³²P-labelled pDNA (0–1 μg/ml) at 37° (closed square) or 4° (open circle). Each point represents the mean ± standard deviation (n = 3). (e and f) Cells were incubated at 4° for 30 min in the presence of 5 μg/ml Texas Red-labelled pDNA. After washing, the cells were warmed to 37° to allow internalization for 15 min. Images represent laser-scanning confocal microscopy sections.

50% precipitation occurs with the 16-mer oligodeoxynucleotides.³² Both RAW264.7 cells and resident Mφs degraded the pDNA and released its degradation products into the medium to a similar extent (Fig. 6).

Single-stranded DNA or smaller DNA was unable to induce TNF-α production from peritoneal Mφs

Resident peritoneal Mφs were found to induce inflammatory cytokines by a small single-stranded CpG ODN (Fig. 4a),

although they were unable to produce TNF-α following stimulation with larger double-stranded pDNA (Fig. 1). *E. coli* DNA is often used after sonication and heat denaturation.^{3,5,7,33,34} We prepared small DNA fragments by sonication to examine whether the physicochemical properties of DNA affect the activation of Mφs. pDNA fragments were reduced to less than 600 bp after sonication for 120 min (Fig. 7). In addition, pDNA, or its fragments, were denatured at 90° to prepare single-stranded DNA. In RAW264.7 cells, the amount of TNF-α released by DNA fragments was almost the same as

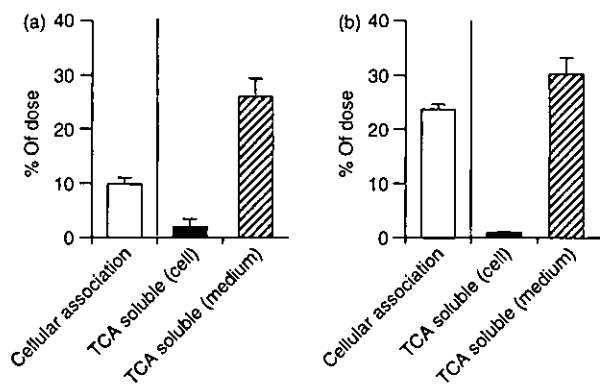


Figure 6. Degradation of ³²P-labelled plasmid DNA (pDNA) by RAW264.7 cells (a) or resident macrophages (b). The cells were incubated with ³²P-labelled pDNA (0–1 μg/ml) at 37° or 4° for 3 hr. The degree of cellular association and degradation of ³²P-labelled pDNA was measured by the trichloroacetic acid (TCA) precipitation method. Each result represents the mean and standard deviation (n = 6).

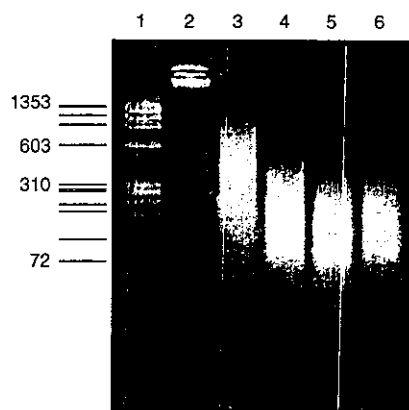


Figure 7. Electrophoresis of plasmid DNA (pDNA) fragments prepared by sonication. DNA mobility was analysed by agarose-gel electrophoresis (3.5% gel). Lane 1, Φ-HaeIII marker; lane 2, control pCMV-Luc; lanes 3–6, pCMV-Luc fragments produced by sonication for 30, 60, 90 and 120 min, respectively.

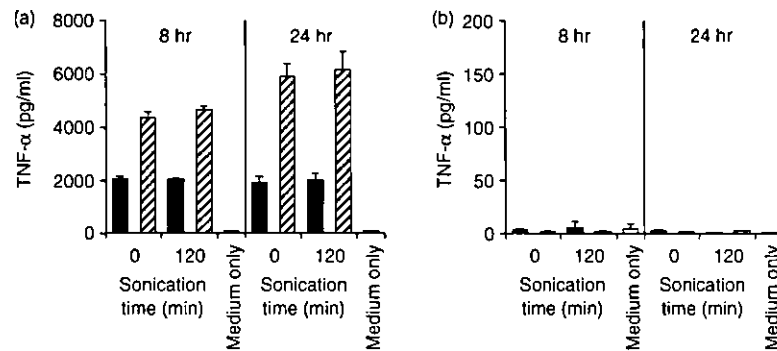


Figure 8. Cytokine release induced by plasmid DNA (pDNA) fragments or single-stranded DNA from RAW264.7 cells (a) or resident macrophages (Mφs) (b). The cells were incubated with double-stranded DNA (black bar) or single-stranded DNA (hatched bar) for 8 hr. Cytokine release from Mφs was quantified by enzyme-linked immunosorbent assay (ELISA). Each result represents the mean and standard deviation ($n = 6$).

that released by intact pDNA (Fig. 8). On the other hand, heat-denatured pDNA significantly increased TNF- α production from the Mφ cell line, indicating that single-stranded DNA is a more potent cell activator. However, resident Mφs could not secrete TNF- α upon stimulation with small-size pDNA or heat-denatured pDNA.

DISCUSSION

The important role of immunostimulatory effects mediated by the CpG motif in gene therapy and DNA vaccination has been well defined. However, most *in vitro* studies, focusing on the mechanisms of Mφ activation mediated by CpG DNA, have been carried out using CpG ODN and bacterial genomic DNA in Mφ cell lines.^{28,35,36} Only a few reports have investigated immune responses induced by pDNA or bacterial DNA from Mφs or monocytes in primary culture.³⁷⁻³⁹

In the present study, we used Triton X-114 to remove LPS from DNA samples. Naked pDNA and *E. coli* genomic DNA containing unmethylated CpG motifs were able to stimulate the Mφ cell lines RAW264.7 and J774A1 to produce a significant amount of TNF- α (Fig. 2), while mammalian calf thymus DNA, which does not contain immunostimulatory CpG motifs, could not stimulate TNF- α production from these cell lines. Inhibitors of endocytosis and endosomal acidification prevented the pDNA-stimulated release of TNF- α from RAW264.7 cells (Fig. 4b). Therefore, it is probable that pDNA activates RAW264.7 cells to secrete cytokines by the same mechanism as that reported for CpG ODN.²⁸

On the other hand, the resident and elicited Mφs from male ICR mice did not show any TNF- α or IL-6 induction by naked pDNA or *E. coli* DNA, even when exposed to a very high concentration of these DNAs (Fig. 1). Similar results were observed in the resident Mφs isolated from female ICR and male C3H/HeJ (LPS non-responders) and C3H/HeN mice (data not shown). Peritoneal Mφs primed by interferon- γ (IFN- γ) also showed similar results, although increased TNF- α secretion induced by LPS was observed in the primed cells (data not shown). This unresponsiveness of primary Mφs disagreed with previous reports.^{5,38} Bone marrow-derived Mφs can respond to pDNA,³⁸ and only 1 μ g/ml pDNA can induce NF- κ B activation

and TNF- α production in such Mφs. It may be that peritoneal Mφs and bone marrow-derived Mφs exhibit different responses to pDNA. Another report shows that DNA from Gram-positive *Staphylococcus aureus* can activate peritoneal Mφs of C3H/HeJ mice to produce TNF- α .⁵ *S. aureus* DNA may contain higher numbers or more potent CpG motifs than Gram-negative *E. coli* DNA or the pDNA that we used. Further studies are required to explain these contradictions. The very low, almost negligible, induction of cytokine upon stimulation with naked DNA was in complete contrast to our recent findings on DNA/cationic liposome complexes.²¹ Both the resident peritoneal Mφs and RAW264.7 cells secreted a large amount of TNF- α following incubation with pDNA and *E. coli* DNA complexed with LipofectAMINE plus. Also of note, similar cytokine induction was evoked in both resident peritoneal Mφs and RAW264.7 cells by the complexes prepared with calf thymus DNA and methylated-CpG pDNA, indicating that the Mφ activation was a CpG motif-independent process.

The restricted induction of cytokines by naked pDNA was not a result of the lack of TLR-9 expression in the peritoneal Mφs (Fig. 3), which is responsible for recognition of the bacterial CpG DNA.^{14,15} Indeed, the Mφ can release TNF- α in a CpG motif-dependent manner (Fig. 4), as previously reported.^{4,38} Therefore, the resident Mφs have the ability to respond to CpG DNA.

CpG DNA should be taken up by Mφs and, thereafter, be transported to the endosomal/lysosomal compartment for recognition by TLR-9.³⁰ pDNA was efficiently taken up and degraded into smaller DNA fragments by the resident peritoneal Mφs (Figs 5 and 6). The pDNA degradation would be mediated by DNase II in the lysosomal compartment of the Mφs.^{31,40,41} However, the apparent uptake efficiency of pDNA by the resident Mφs appeared to be higher than that of RAW264.7 cells. Therefore, the very low responsiveness to pDNA was not a result of impaired cellular uptake of the CpG DNA by the peritoneal Mφs.

In cellular activation experiments, *E. coli* DNA is often used after sonication and heat denaturation.^{3,5,7,33,34} Heat-denatured (single-stranded) *E. coli* DNA was 10–30% more mitogenic than double-stranded DNA as far as B cells were concerned.³⁴ In fact, in the present study, RAW264.7 cells were stimulated to

produce about twice as much TNF- α by single-stranded pDNA compared with double-stranded pDNA (Fig. 8a). On the other hand, DNA fragments prepared by sonication resulted in a similar level of TNF- α secretion compared with control pDNA. This was in agreement with a previous report that mycobacterial DNA fragments generated by digestion with restriction enzyme or the fragments prepared by sonication do not modify IL-12 induction by THP-1 monocytes.⁴² Heat-denatured single-stranded pDNA, which exhibited a greater ability to induce TNF- α in RAW264.7 cells, could not stimulate resident M ϕ s to induce inflammatory cytokines (Fig. 8a).

The findings of the present study suggest that peritoneal M ϕ s, or other M ϕ s such as Kupffer cells, may play an insignificant role in cytokine production through direct activation by naked pDNA *in vivo*. pDNA is efficiently taken up by the liver when it is injected into mice, and hepatic accumulation has been found to occur preferentially in the non-parenchymal cells, including Kupffer cells (liver M ϕ s).¹⁸ When mice are sensitized with D-galactosamine they suffer from lethal toxic shock as a result of TNF- α , induced by bacterial DNA, producing fulminant apoptosis of liver cells.⁵ However, a very large dose (300 μ g/mouse) is required to produce this shock. Moreover, bacterial DNA alone is less toxic and cannot induce lethal shock without LPS or D-galactosamine treatment.⁴³ These observations are in agreement with our speculation involving restricted cytokine production by direct pDNA stimulation from M ϕ s *in vivo*.

The restricted cytokine induction by naked pDNA also contrasts with our recent observation of DCs in culture. Significant production of inflammatory cytokines, such as TNF- α , IL-6 and IL-12, was induced by naked pDNA and *E. coli* DNA, but not by calf thymus DNA, from both bone marrow-derived DCs in primary culture and a DC cell line, DC2.4.⁴⁴ Neither type of DC displayed CpG motif-independent cytokine secretion upon stimulation with DNA/cationic liposome complexes. Therefore, DCs, another important cell population for DNA-based therapies, show CpG motif-dependent cytokine production against pDNA, regardless of whether the cells are in primary culture or of a cell line. M ϕ s have features distinct from DCs in terms of cytokine induction by pDNA.

In conclusion, the present study demonstrated that primary cultured mouse peritoneal M ϕ s and M ϕ cell lines exhibit significantly different responses to pDNA as far as inflammatory cytokine induction is concerned. In contrast to the cell lines, the peritoneal M ϕ s secreted almost no inflammatory cytokines (TNF- α , IL-6) upon stimulation with pDNA, in spite of extensive uptake of the CpG DNA. These findings have important implications for M ϕ activation by naked pDNA in DNA-based therapies because it has been generally assumed that pDNA-containing CpG motifs are potent agents for inducing inflammatory cytokines *in vivo* based on information from *in vitro* studies using M ϕ cell lines.

ACKNOWLEDGMENTS

This work was supported in part by a grant-in-aid for Scientific Research from the Ministry of Education, Culture, Sports, Sciences and Technology, Japan.

REFERENCES

- Krieg AM, Kline JN. Immune effects and therapeutic applications of CpG motifs in bacterial DNA. *Immunopharmacology* 2000; **48**:303.
- Wagner H. Immunobiology of Bacterial CpG-DNA. In: Wagner H, ed. *Current Topics in Microbiology and Immunology*, Vol 247. Berlin: Springer, 1999.
- Yi AK, Klinman DM, Martin TL, Matson S, Krieg AM. Rapid immune activation by CpG motifs in bacterial DNA. Systemic induction of IL-6 transcription through an antioxidant-sensitive pathway. *J Immunol* 1996; **157**:5394.
- Sparwasser T, Miethke T, Lipford G, Borschert K, Hacker H, Heeg K, Wagner H. Bacterial DNA causes septic shock. *Nature* 1997; **386**:336.
- Sparwasser T, Miethke T, Lipford G, Erdmann A, Hacker H, Heeg K, Wagner H. Macrophages sense pathogens via DNA motifs: induction of tumor necrosis factor- α -mediated shock. *Eur J Immunol* 1997; **27**:1671.
- Krieg AM, Love HL, Yi AK, Harty JT. CpG DNA induces sustained IL-12 expression *in vivo* and resistance to *Listeria monocytogenes* challenge. *J Immunol* 1998; **161**:2428.
- Klinman DM, Yi AK, Beauce SL, Conover J, Krieg AM. CpG motifs present in bacteria DNA rapidly induce lymphocytes to secrete interleukin 6, interleukin 12, and interferon gamma. *Proc Natl Acad Sci USA* 1996; **93**:2879.
- Singh M, O'Hagan D. Advances in vaccine adjuvants. *Nat Biotechnol* 1999; **17**:1075.
- Weeratna RD, McCluskie MJ, Xu Y, Davis HL. CpG DNA induces stronger immune responses with less toxicity than other adjuvants. *Vaccine* 2000; **18**:1755.
- Raz E, Tighe H, Sato Y *et al*. Preferential induction of a Th1 immune response and inhibition of specific IgE antibody formation by plasmid DNA immunization. *Proc Natl Acad Sci USA* 1996; **93**:5141.
- Roman M, Martin OE, Goodman JS *et al*. Immunostimulatory DNA sequences function as T helper-1-promoting adjuvants. *Nat Med* 1997; **3**:849.
- Qin L, Ding Y, Pahud DR, Chang E, Imperiale MJ, Bromberg JS. Promoter attenuation in gene therapy: interferon-gamma and tumor necrosis factor- α inhibit transgene expression. *Hum Gene Ther* 1997; **8**:2019.
- Ghazizadeh S, Carroll JM, Taichman LB. Repression of retrovirus-mediated transgene expression by interferons: implications for gene therapy. *J Virol* 1997; **71**:9163.
- Hemmi H, Takeuchi O, Kawai T *et al*. A Toll-like receptor recognizes bacterial DNA. *Nature* 2000; **408**:740.
- Bauer S, Kirschning CJ, Hacker H, Redecke V, Hausmann S, Akira S, Wagner H, Lipford GB. Human TLR9 confers responsiveness to bacterial DNA via species-specific CpG motif recognition. *Proc Natl Acad Sci USA* 2001; **98**:9237.
- Hacker H, Vabulas RM, Takeuchi O, Hoshino K, Akira S, Wagner H. Immune cell activation by bacterial CpG-DNA through myeloid differentiation marker 88 and tumor necrosis factor receptor-associated factor (TRAF) 6. *J Exp Med* 2000; **192**:595.
- Baud V, Liu ZG, Bennett B, Suzuki N, Xia Y, Karin M. Signaling by proinflammatory cytokines: oligomerization of TRAF2 and TRAF6 is sufficient for JNK and IKK activation and target gene induction via an amino-terminal effector domain. *Genes Dev* 1999; **13**:1297.
- Kawabata K, Takakura Y, Hashida M. The fate of plasmid DNA after intravenous injection in mice: involvement of scavenger receptors in its hepatic uptake. *Pharm Res* 1995; **12**:825.
- Takagi T, Hashiguchi M, Mahato RI, Tokuda H, Takakura Y, Hashida M. Involvement of specific mechanism in plasmid DNA

- uptake by mouse peritoneal macrophages. *Biochem Biophys Res Commun* 1998; **245**:729.
- 20 Takakura Y, Takagi T, Hashiguchi M *et al.* Characterization of plasmid DNA binding and uptake by peritoneal macrophages from class A scavenger receptor knockout mice. *Pharm Res* 1999; **16**:503.
 - 21 Yasuda K, Ogawa Y, Kishimoto M, Takagi T, Hashida M, Takakura Y. Plasmid DNA activates murine macrophages to induce inflammatory cytokines in a CpG motif-independent manner by complex formation with cationic liposomes. *Biochem Biophys Res Commun* 2002; **293**:344.
 - 22 Nomura T, Yasuda K, Yamada T, Okamoto S, Mahato RI, Watanabe Y, Takakura Y, Hashida M. Gene expression and antitumor effects following direct interferon (IFN)-gamma gene transfer with naked plasmid DNA and DC-chol liposome complexes in mice. *Gene Ther* 1999; **6**:121.
 - 23 Rigby PW, Dieckmann M, Rhodes C, Berg P. Labeling deoxyribonucleic acid to high specific activity *in vitro* by nick translation with DNA polymerase I. *J Mol Biol* 1977; **113**:237.
 - 24 Cotten M, Baker A, Saltik M, Wagner E, Buschle M. Lipopolysaccharide is a frequent contaminant of plasmid DNA preparations and can be toxic to primary human cells in the presence of adenovirus. *Gene Ther* 1994; **1**:239.
 - 25 Hartmann G, Krieg AM. CpG DNA and LPS induce distinct patterns of activation in human monocytes. *Gene Ther* 1999; **6**:893.
 - 26 Krieg AM, Yi AK, Matson S, Waldschmidt TJ, Bishop GA, Teasdale R, Koretzky GA, Klinman DM. CpG motifs in bacterial DNA trigger direct B-cell activation. *Nature* 1995; **374**:546.
 - 27 Wang C, Smith RL. Lowry determination of protein in the presence of Triton X-100. *Anal Biochem* 1975; **63**:414.
 - 28 Yi AK, Tuetken R, Redford T, Waldschmidt M, Kirsch J, Krieg AM. CpG motifs in bacterial DNA activate leukocytes through the pH-dependent generation of reactive oxygen species. *J Immunol* 1998; **160**:4755.
 - 29 Hacker H, Mischak H, Miethke T *et al.* CpG-DNA-specific activation of antigen-presenting cells requires stress kinase activity and is preceded by non-specific endocytosis and endosomal maturation. *EMBO J* 1998; **17**:6230.
 - 30 Ahmad-Nejad P, Hacker H, Rutz M, Bauer S, Vabulas RM, Wagner H. Bacterial CpG-DNA and lipopolysaccharides activate Toll-like receptors at distinct cellular compartments. *Eur J Immunol* 2002; **32**:1958.
 - 31 Krieser RJ, Eastman A. The cloning and expression of human deoxyribonuclease II. A possible role in apoptosis. *J Biol Chem* 1998; **273**:30909.
 - 32 Cleaver JE, Boyer HW. Solubility and dialysis limits of DNA oligonucleotides. *Biochim Biophys Acta* 1972; **262**:116.
 - 33 Schwartz DA, Quinn TJ, Thome PS, Sayeed S, Yi AK, Krieg AM. CpG motifs in bacterial DNA cause inflammation in the lower respiratory tract. *J Clin Invest* 1997; **100**:68.
 - 34 Sun S, Beard C, Jaenisch R, Jones P, Sprent J. Mitogenicity of DNA from different organisms for murine B cells. *J Immunol* 1997; **159**:3119.
 - 35 Sester DP, Stacey KJ, Sweet MJ, Beasley SJ, Cronau SL, Hume DA. The actions of bacterial DNA on murine macrophages. *J Leukoc Biol* 1999; **66**:542.
 - 36 Gao JJ, Zuvanich EG, Xue Q, Horn DL, Silverstein R, Morrison DC. Cutting edge: bacterial DNA and LPS act in synergy in inducing nitric oxide production in RAW264.7 macrophages. *J Immunol* 1999; **163**:4095.
 - 37 Sweet MJ, Stacey KJ, Kakuda DK, Markovich D, Hume DA. IFN-gamma primes macrophage responses to bacterial DNA. *J Interferon Cytokine Res* 1998; **18**:263.
 - 38 Stacey KJ, Sweet MJ, Hume DA. Macrophages ingest and are activated by bacterial DNA. *J Immunol* 1996; **157**:2116.
 - 39 Bauer M, Heeg K, Wagner H, Lipford GB. DNA activates human immune cells through a CpG sequence-dependent manner. *Immunology* 1999; **97**:699.
 - 40 Odaka C, Mizuochi T. Role of macrophage lysosomal enzymes in the degradation of nucleosomes of apoptotic cells. *J Immunol* 1999; **163**:5346.
 - 41 McIlroy D, Tanaka M, Sakahira H *et al.* An auxiliary mode of apoptotic DNA fragmentation provided by phagocytes. *Genes Dev* 2000; **14**:549.
 - 42 Filion MC, Filion B, Reader S, Menard S, Phillips NC. Modulation of interleukin-12 synthesis by DNA lacking the CpG motif and present in a mycobacterial cell wall complex. *Cancer Immunol Immunother* 2000; **49**:325.
 - 43 Cowdery JS, Chace JH, Yi AK, Krieg AM. Bacterial DNA induces NK cells to produce IFN-gamma *in vivo* and increases the toxicity of lipopolysaccharides. *J Immunol* 1996; **156**:4570.
 - 44 Yoshinaga T, Yasuda K, Ogawa Y, Takakura Y. Efficient uptake and rapid degradation of plasmid DNA by murine dendritic cells via a specific mechanism. *Biochem Biophys Res Commun* 2002; **299**:389.

Inhibition of Metastatic Tumor Growth in Mouse Lung by Repeated Administration of Polyethylene Glycol-Conjugated Catalase: Quantitative Analysis with Firefly Luciferase-Expressing Melanoma Cells

Kenji Hyoudou,¹ Makiya Nishikawa,²
Yukari Umeyama,¹ Yuki Kobayashi,¹
Fumiyoshi Yamashita,¹ and Mitsuru Hashida¹

Department of ¹Drug Delivery Research, and ²Biopharmaceutics and Drug Metabolism, Graduate School of Pharmaceutical Sciences, Kyoto University, Kyoto, Japan

ABSTRACT

Purpose: To develop a novel and effective approach to inhibit tumor metastasis based on controlled delivery of catalase, we first evaluated the characteristics of the disposition and proliferation of tumor cells. Then, we examined the effects of polyethylene glycol-conjugated catalase (PEG-catalase) on tumor metastasis. On the basis of the results obtained, PEG-catalase was repetitively administered to completely suppress the growth of tumor cells.

Experimental Design: Murine melanoma B16-BL6 cells were stably transfected with firefly luciferase gene to obtain B16-BL6/Luc cells. These cells were injected intravenously into syngeneic C57BL/6 mice. PEG-catalase was injected intravenously, and the effect was evaluated by measuring the luciferase activity as the indicator of the number of tumor cells.

Results: At 1 hour after injection of B16-BL6/Luc cells, 60 to 90% of the injected cells were recovered in the lung. The numbers decreased to 2 to 4% at 24 hours, then increased. An injection of PEG-catalase just before inoculation significantly reduced the number of tumor cells at 24 hours. Injection of PEG-catalase at 1 or 3 days after inoculation was also effective in reducing the cell numbers. Daily dosing of PEG-catalase greatly inhibited the proliferation

and the number assayed at 14 days after inoculation was not significantly different from the minimal number observed at 1 day, suggesting that the growth had been markedly suppressed by the treatment.

Conclusions: These findings indicate that sustained catalase activity in the blood circulation can prevent the multiple processes of tumor metastasis in the lung, which could lead to a state of tumor dormancy.

INTRODUCTION

Tumor metastasis is the major cause of death in cancer patients. It can be roughly divided into the following steps: tumor cell dissociation, invasion, intravasation, distribution to distant organs, arrest in small vessels, adhesion to endothelial cells, extravasation, invasion of the target organ and proliferation (1). Adhesion of circulating tumor cells to capillary endothelial cells is a crucial event in the retention of tumor cells in a specific organ (2). Initial interactions between tumor cells and endothelium activates both tumor cells and endothelial cells through cytokines, free radicals, bioactive lipids, and growth factors, leading to the increased expression of adhesion molecules, which strengthens the initial adhesive bonds (3, 4). Reactive oxygen species (ROS), such as hydrogen peroxide (H₂O₂), superoxide anion and hydroxyl radical, are well known regulators of such adhesion molecules (5-7).

In most cases, the lung is the first organ that tumor cells detached from primary tumors encounter, making it a major site for tumor metastasis. We have shown that an experimental pulmonary metastasis of colon carcinoma cells in mice can be effectively inhibited by polyethylene glycol-conjugated catalase (PEG-catalase; ref. 8). The number of metastatic colonies on the lung surface was significantly lower in mice treated with PEG-catalase than in untreated (saline-injected) mice. However, the mechanism of this inhibition is not clear because ROS are involved in various metastatic processes, such as adhesion (5, 6), invasion (9-11), and proliferation (12). Counting visible metastatic colonies on the tissue surface is not sensitive enough to evaluate these early processes of tumor metastasis. In an attempt to circumvent this problem, radiolabeled tumor cells are sometimes used to trace their disposition *in vivo*, but cell death as well as the release of radiolabeled compounds from cells make it very difficult to analyze the disposition of tumor cells. Furthermore, tumor growth cannot be evaluated by this approach.

Labeling of cells with any protein by introducing its gene has been applied to studies of tumor metastasis. This technique is very promising in evaluating tumor metastasis because the protein introduced can be tumor cell-specific. Thus far, several authors have already used this kind of experimental system to

Received 5/25/04; revised 7/24/04; accepted 7/29/04.

Grant support: Grants-in-Aid for Scientific Research from the Ministry of Education, Culture, Sports, Science, and Technology of Japan (No. 15025233), by Health and Labor Sciences Research Grants for Research on Hepatitis and Bovine Spongiform Encephalopathy from the Ministry of Health, Labor, and Welfare of Japan (No. 15-21) and by the 21st Century Center of Excellence Program "Knowledge Information Infrastructure for Genome Science."

The costs of publication of this article were defrayed in part by the payment of page charges. This article must therefore be hereby marked advertisement in accordance with 18 U.S.C. Section 1734 solely to indicate this fact.

Requests for reprints: Mitsuru Hashida, Department of Drug Delivery Research, Graduate School of Pharmaceutical Sciences, Kyoto University, Sakyo-ku, Kyoto, Japan. Phone: 81-75-753-4545; Fax: 81-75-753-4575; E-mail: hashidam@pharm.kyoto-u.ac.jp.

©2004 American Association for Cancer Research.

show the growth of tumor cells *in vivo* (13, 14) and metastasis by *in vivo* imaging (14–17). However, there have been few investigations of the early processes of tumor metastasis, such as the embolization, adhesion, and invasion, using these reporter gene-labeled tumor cells. These processes cannot be evaluated by *in vivo* imaging because of a lack of sensitivity and its less quantitative nature. Reporter gene assays can solve these problems if tumor cells are stably transfected at a high level of specific activity. In addition, the reporter gene expression should be constant under a variety of conditions to use the activity as a scale for the number of tumor cells *in vivo*.

In the present study, we first developed clones of murine melanoma B16-BL6 cells by transfecting firefly luciferase gene. The characteristics of the transfectant, B16-BL6/Luc cells, were examined *in vitro* as well as *in vivo*, and we found that the transfectant can be used to examine the disposition and proliferation of tumor cells *in vivo*. Therefore, the processes of tumor metastasis were examined in mice by measuring the luciferase activity in the lung after intravenous administration of the cells. Finally, the effects of catalase and PEG-catalase on early as well as later processes of tumor metastasis were evaluated in this system. To our knowledge, this is the first report showing that repeated injection of PEG-catalase almost completely suppresses the growth of metastatic tumors in the lung. These findings suggest that tumor dormancy may be induced by continuous administration of PEG-catalase.

MATERIALS AND METHODS

Animals. Male C57/BL6 (6-week-old) mice were purchased from the Shizuoka Agricultural Cooperative Association for Laboratory Animals (Shizuoka, Japan). Animals were maintained under conventional housing conditions. All animal experiments were conducted in accordance with the principles and procedures outlined in the United States NIH Guide for the Care and Use of Laboratory Animals. The protocols for animal experiments were approved by the Animal Experimentation Committee of Graduate School of Pharmaceutical Sciences of Kyoto University.

Chemicals. DMEM and HBSS were obtained from Nissui Pharmaceutical (Tokyo, Japan). Fetal bovine serum was obtained from Biowhitaker (Walkersville, MD). Bovine liver catalase (C-100, 40,000 units/mg) was purchased from Sigma Chemical (St. Louis, MO). A product of PEG [2,4-bis (*o*-methoxypolyethylene glycol)-6-chloro-*s*-triazin] was obtained from Seikagaku Corporation (Japan), and PEG-catalase and inactivated catalase were synthesized and their enzymatic activity measured as reported previously (18). All other chemicals were of the highest grade commercially available.

Tumor Cells. Murine melanoma B16-BL6 tumor cells (19), obtained from the Cancer Chemotherapy Center of the Japanese Foundation for Cancer Research (Tokyo, Japan), were grown in DMEM supplemented with 10% heat-inactivated fetal bovine serum, 0.15% NaHCO₃, 100 units/mL penicillin, and 100 μg/mL streptomycin at 37°C in humidified air containing 5% CO₂. To establish cell lines stably expressing firefly luciferase, B16-BL6 cells were transfected with plasmid DNA encoding firefly luciferase under the control of cytomegalovirus immediate early promoter (20) complexed with Lipo-

fectamine2000 (Life Technologies, Inc.—Invitrogen). Then the cells were treated with medium containing 1 mg/mL G418 (Geneticin, Sigma) and single colonies of G418-resistant cells were picked up and examined for their luciferase activity as described below. On the basis of the luciferase activity, a clone was selected and its growth rate *in vitro* was compared with that of B16-BL6 cells. In addition, 1 × 10⁵ cells of B16-BL6 or B16-BL6/Luc were injected into the lateral tail vein of mice. At 2 weeks after injection, the number of metastatic colonies on the lung surface was counted.

Disposition and Proliferation of B16-BL6/Luc Cells after Intravenous Injection in Mice. Into the lateral tail vein of mice were injected 1 × 10³, 1 × 10⁴, 1 × 10⁵, 5 × 10⁵ or 1 × 10⁶ B16-BL6/Luc cells in 0.1 mL HBSS. At 1, 24 hours, 3, 7, and 14 days after tumor injection, mice were killed and the lung was excised, weighed, and the luciferase activity in the tissue was measured.

Effect of Catalase Derivatives on the Number of B16-BL6/Luc Cells in Mice. Experimental pulmonary metastasis was induced by injecting 1 or 5 × 10⁵ B16-BL6/Luc cells in 0.1 mL of HBSS into the lateral tail vein of C57/BL6 mice. Saline (untreated, control group), catalase, PEG-catalase, or inactivated catalase was injected in the lateral tail vein at a dose of 1,000 catalase units unless otherwise indicated. At 24 hours after tumor injection, mice were killed, and the lung was excised, weighed, and the luciferase activity in the tissue was measured.

Separately, the effects of catalase on tumor metastasis at later periods were examined by measuring the luciferase activity of the lung at 7 days after tumor injection. Experimental pulmonary metastasis was induced by injecting 1 × 10⁵ B16-BL6/Luc cells as described above. Then, saline or PEG-catalase was injected just before, and 1 or 3 days after tumor injection.

Multiple Dosing of PEG-Catalase. Experimental pulmonary metastasis was induced by injecting 1 × 10⁴ B16-BL6/Luc cells in 0.1 mL of HBSS into the lateral tail vein of C57/BL6 mice. Saline (untreated, control group) or PEG-catalase was injected daily into the lateral tail vein at a dose of 1,000 catalase units/injection. At 2 weeks after tumor injection, mice were killed, and the lungs were excised, weighed, and the luciferase activity in the tissues was measured.

Separately, the effects of PEG-catalase on the survival of mice with lung metastases were examined. Experimental pulmonary metastasis was induced by injecting 1 × 10⁴ B16-BL6/Luc cells as described above. Then, saline, PEG-catalase (1,000 catalase units), or bovine serum albumin (BSA; amount of protein equivalent to PEG-catalase) was injected daily into the lateral tail vein until 30 days after tumor injection.

Measurement of Luciferase Activity. The cells or tissues were homogenized with a lysis buffer [0.05% Triton X-100, 2 mmol/L EDTA, 0.1 mol/L Tris (pH 7.8)], and subjected to three cycles of freezing (liquid N₂ for 3 minutes) and thawing (37°C, 3 minutes), followed by centrifugation at 10,000 × g for 10 minutes. Ten microliters of the supernatant was mixed with 100 μL of luciferase assay buffer (Picagene, Toyo Ink, Tokyo, Japan), and the light produced was immediately measured with a luminometer (Lumat LB 9507, EG & G Berthold, Bad Wildbad, Germany).

Statistical Analysis. Differences were statistically evaluated by one-way ANOVA followed by the Student-Newmann-

Keuls multiple comparison test and Kaplan-Meier analysis with a log-rank test to determine survival, and the level of statistical significance was $P < 0.05$.

RESULTS

Characteristics of B16-BL6/Luc Cells. A number of B16-BL6/Luc colonies were obtained with different levels of luciferase activity. A colony expressing high luciferase activity was selected, and the characteristics of the cells were examined. There was no significant difference in the growth rates of B16-BL6 and B16-BL6/Luc cells *in vitro* (data not shown). In addition, they were microscopically identical. When injected into the tail vein of mice, both types of cell induced comparable numbers of metastatic colonies at 14 days (5 ± 1 for B16-BL6 cells and 6 ± 2 for B16-BL6/Luc cells, $P > 0.05$). These results indicate that the characteristics of B16-BL6 cells are hardly altered during the procedure for preparing B16-BL6/Luc cells.

The luciferase activity was proportional to the number of cells [relative light units (RLU)/cell] over a wide range from 100 RLU to 10,000,000 RLU. Treatment of the cultured B16-BL6/Luc cells with H_2O_2 (10 $\mu\text{mol/L}$) or catalase (10,000 units/mL) for up to 7 hours hardly altered the luciferase activity of the cells (data not shown). The expression level of luciferase in the clone was stable for up to 1 year.

Disposition and Proliferation of B16-BL6/Luc Cells in Mouse Lung. The lung excised from untreated mice showed no significant luciferase activity (< 100 RLU/10 μL of sample). The addition of B16-BL6/Luc cells to lung tissues proportionally increased the luciferase activity according to the number of the cells (data not shown), indicating that the luciferase activity of the tissue can be used as an indicator of the number of cells. On the basis of these findings, the luciferase activity measured was converted to the number of B16-BL6/Luc cells in the lung. The regression line gave a constant of 50 RLU/cell for the quantification of the number of tumor cells. Measuring the luciferase activity of lung homogenates mixed with B16-BL6/Luc cells showed that ≥ 60 cells were enough for the detection of B16-BL6/Luc cells (Fig. 1).

Figure 2 shows the number of B16-BL6/Luc cells in the lungs of mice after intravenous injection of different numbers of

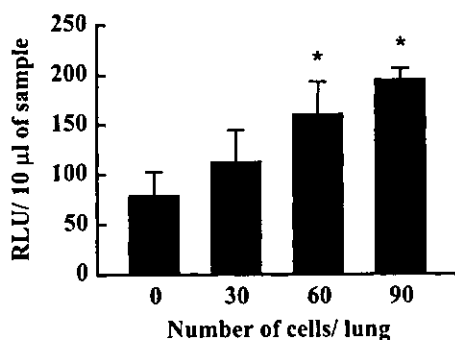


Fig. 1 Luciferase activity in the supernatant of homogenates of mouse lung mixed with different numbers of B16-BL6/Luc cells. Results are expressed as the mean \pm SD of three samples. *, a statistically significant difference compared with the mouse lung without tumor cells ($P < 0.001$).

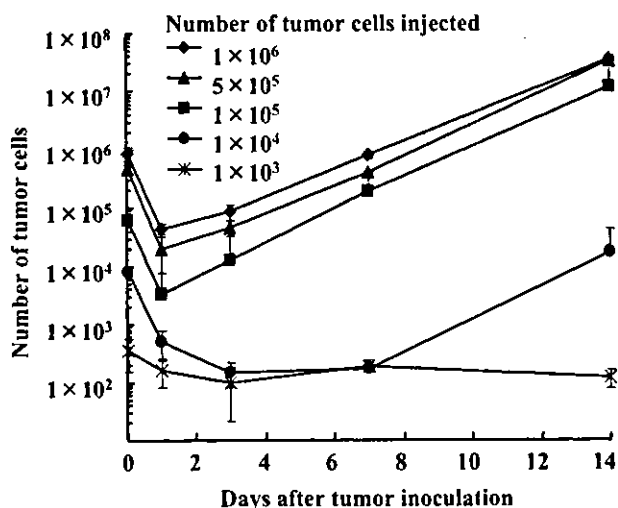


Fig. 2 Number of tumor cells in mouse lung after inoculation of B16-BL6/Luc cells into the tail vein at numbers of 1×10^6 , 5×10^5 , 1×10^5 , 1×10^4 , or 1×10^3 B16-BL6/Luc cells. Results are expressed as the mean \pm SD of at least 3 mice.

cells. At 1 hours, about 60 to 90% of the luciferase activity derived from the injected cells was recovered in the lung. Little luciferase activity was detected in other organs such as the liver and spleen (data not shown). At 24 hours, however, only 2 to 4% of the injected cells were detected in the lung. Thereafter, when $\geq 1 \times 10^5$ cells were injected, the number of tumor cells in the lung increased with time. However, the growth of the tumor cells was rather slow when small numbers of cells were injected. When mice were injected with 1×10^3 cells, the number of cells in the lung hardly changed with time up to 14 days.

Effect of Catalase Derivatives on the Number of B16-BL6/Luc Cells in Mouse Lung at 24 hours. It was found that the number of tumor cells was minimal at 24 hours after injection of B16-BL6/Luc cells. Then, we investigated whether catalase derivatives were able to reduce the number of tumor cells as early as 24 hours after the intravenous injection of 1×10^5 B16-BL6/Luc cells (Fig. 3A). An intravenous injection of catalase at a dose of 1,000 units/mouse tended to reduce the number of the tumor cells in the lung from 1.5×10^4 cells to 1.1×10^4 cells, but the difference was not significant. However, PEG-catalase had a greater inhibitory effect on the number of the tumor cells in the lung than catalase; only 0.50×10^4 cells were detected at 24 hours after tumor injection ($P < 0.05$ compared with the saline-treatment or catalase-treatment group).

In a separate set of experiments, PEG-catalase was injected at doses ranging from 100 to 10,000 units/mouse. The lowest dose of PEG-catalase was also effective in reducing the number of tumor cells in the lung (Fig. 3B). The number of the cells in the lung was proportional to the dose of PEG-catalase, suggesting that the detoxification of H_2O_2 inhibits the tumor cell survival in the lung. Inactivated catalase injected at a dose equivalent to 10,000 units catalase had no effect on metastasis.

Effect of Catalase on the Number of B16-BL6/Luc Cells in Mouse Lung at 7 Days. As shown in Fig. 2, the tumor cells in the lung were in a logarithmic growth phase at 24 h or later.

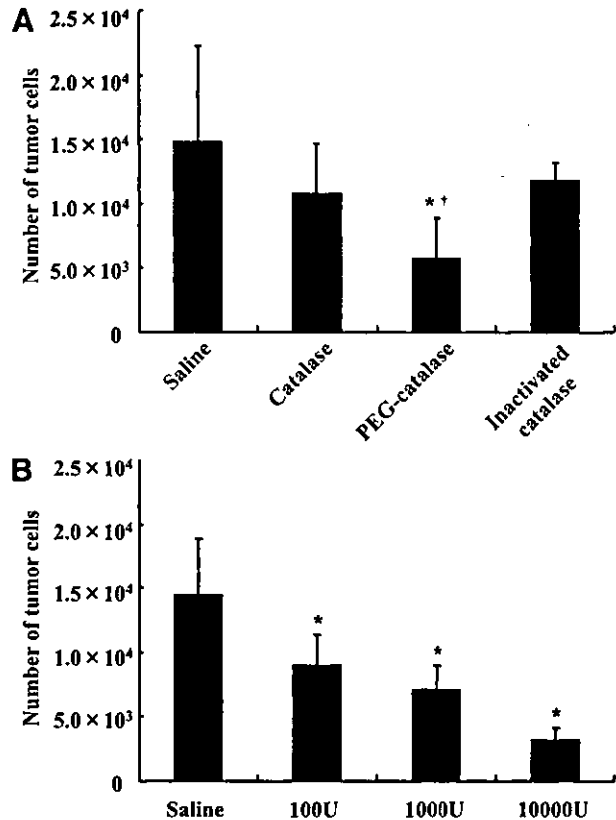


Fig. 3 Effect of catalase derivatives on the number of B16-BL6/Luc cells in mouse lung at 24 hours after inoculation of B16-BL6/Luc cells (5×10^5 cells) into the tail vein. Mice were killed at 24 hours after tumor injection and the luciferase activity in the lung was assayed. Results are expressed as the mean + SD of at least 6 mice. **A**, saline (vehicle), catalase, PEG-catalase (1,000 units/mouse) or inactivated catalase was injected into the tail vein of mice just before the injection of B16-BL6/Luc cells. *, a statistically significant difference compared with the saline group ($P < 0.05$); †, a statistically significant difference compared with the catalase group ($P < 0.05$). **B**, saline (vehicle) or PEG-catalase (100, 1,000, 10,000 units/mouse) was intravenously injected into mice just before the injection of B16-BL6/Luc cells. *, a statistically significant difference compared with the saline group ($P < 0.01$).

Therefore, at any time point around 24 h after injection, the tumor cells that survived appeared to adhere already to the endothelial cells and be ready for invasion and proliferation. To examine the effect of catalase on these tumor metastatic processes, PEG-catalase was injected at 1 or 3 days after tumor injection and the number of the tumor cells was measured at 7 days (Fig. 4). An intravenous injection of PEG-catalase at a dose of 1,000 units/mouse significantly reduced the number of tumor cells in the lung in both cases ($P < 0.005$ compared with the saline-treatment group). In addition, triple injections of PEG-catalase (total 3,000 units/mouse) further reduced the number of tumor cells ($P < 0.05$ compared with any other group), suggesting that the inhibitory effects of PEG-catalase at different periods are additive.

Inhibition of Tumor Cell Growth in Mouse Lung by Daily Injection of PEG-Catalase. It was found that PEG-catalase inhibits not only the early processes of metastasis, such

as the adhesion of tumor cells, but also later processes like invasion and proliferation. Then, we investigated whether multiple injections of PEG-catalase were able to inhibit the growth of metastatic tumor cells in the lung. To the mice given an intravenous injection of 1×10^4 B16-BL6/Luc cells, PEG-catalase was injected at a dose of 1,000 units/injection each day from day 0 to day 14. This treatment resulted in a few tumor cells in the lung at 14 days after tumor inoculation (Fig. 5A). Furthermore, compared with the results of Fig. 2, the number of the cells in the lung of PEG-catalase-treated mice was not significantly different from that observed at 24 hours after tumor injection ($P > 0.05$). In addition, no metastatic colonies were seen under a dissecting microscope (Fig. 5B). Therefore, this suggests that the growth of tumor cells in the lung is almost completely inhibited by a daily injection of PEG-catalase.

Figure 6 shows the survival of mice receiving an intravenous injection of 1×10^4 B16-BL6 (parent) cells. Daily injection of PEG-catalase up to 30 days after tumor inoculation significantly prolonged the survival time of mice with B16-BL6 lung metastases compared with the saline- or BSA-treatment group ($P < 0.0001$ for the saline-treatment group, $P < 0.01$ for the BSA-treatment group).

DISCUSSION

Although metastasis is a major target of cancer therapy, it is difficult to treat metastases effectively. One of the major reasons for this is that the tissue disposition of tumor cells *in vivo* is poorly understood even in animal models. Metastasis consists of a number of different processes, such as adhesion, invasion, proliferation, and angiogenesis. Therefore, any inhib-

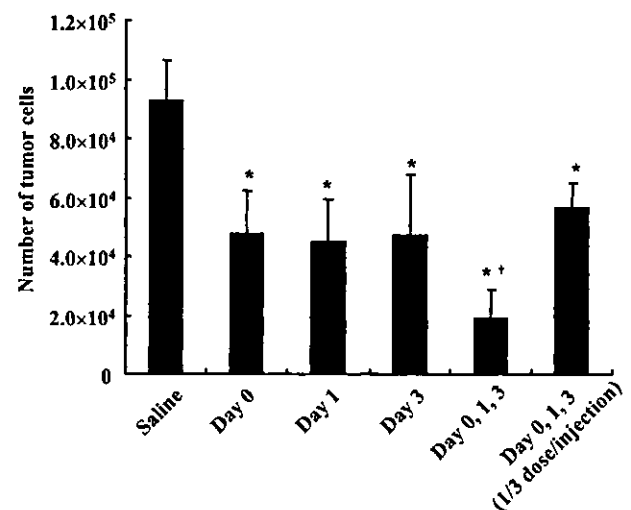


Fig. 4 Effect of injection timing of PEG-catalase on pulmonary metastasis of B16-BL6/Luc cells in mice. Saline (vehicle) or PEG-catalase (1,000 or 333 units/injection) was intravenously injected into mice just before (day 0), or 1 or 3 days after injection of B16-BL6/Luc cells (1×10^5 cells) into the tail vein. Mice were killed at 7 days after tumor injection and the luciferase activity in the lung was assayed. Results are expressed as the mean + SD of at least 6 mice. *, a statistically significant difference compared with the saline group ($P < 0.005$); †, a statistically significant difference compared with any other group ($P < 0.05$).

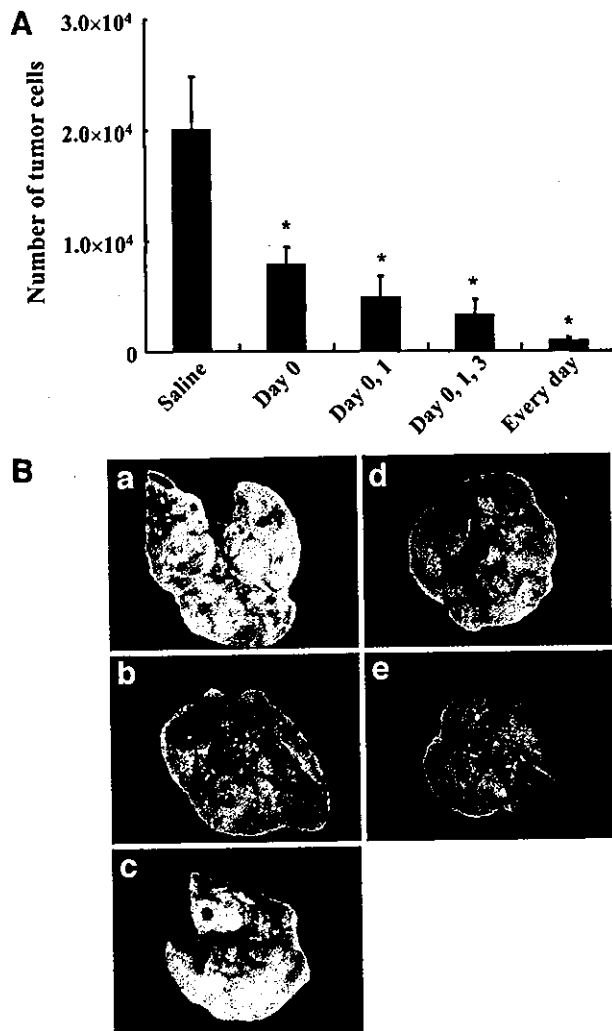


Fig. 5 Effect of multiple dosing of PEG-catalase on pulmonary metastasis in mice. **A**, saline (vehicle) or PEG-catalase (1,000 units/injection) was intravenously injected into mice in the schedule indicated after injection of B16-BL6/Luc cells (1×10^4 cells) into the tail vein. Mice were killed at 14 days after tumor injection and the luciferase activity in the lung was assayed. Results are expressed as the mean + SD of at least 6 mice. *, a statistically significant difference compared with the saline group ($P < 0.001$). **B**, Typical examples of pulmonary metastases in mice receiving an intravenous injection of 1×10^4 B16-BL6/Luc tumor cells followed by an injection of PEG-catalase. (a) Saline (vehicle), (b) PEG-catalase (day 0), (c) PEG-catalase (day 0, 1), (d) PEG-catalase (day 0, 1, 3), (e) PEG-catalase (every day). Each catalase derivative was injected into the tail vein at a dose of 1,000 units/injection.

itor of one of these processes could be an antimetastatic compound. Because the metastatic event results from interactions between tumor cells and other cells, methods analyzing the tissue disposition of tumor cells need to be developed to establish effective approaches for treating tumor metastasis. To this end, we introduced *firefly luciferase* gene into B16-BL6 cells as a marker, and established a highly sensitive and quantitative method to analyze the tissue disposition of tumor cells. Although the use of reporter gene-labeled tumor cells is not a novel approach to studying tumor growth and metastasis, until

now there has been little published information on the separate processes of tumor metastasis. Therefore, in this study, we first examined the tissue disposition of B16-BL6/Luc cells after intravenous injection and identified the characteristic features of the *in vivo* fate of the cells. Then, we applied this analytical system to elucidate the mechanism whereby PEG-catalase reduces the number of metastatic colonies in the lung.

There are several requirements for the transfectant to use the luciferase activity in tissues as an indicator of the number of tumor cells. First, the expression level of luciferase should be high enough to ensure that a few cells can be detected *in vivo*. Second, the expression must be stable for a long period even after inoculation in mice. Furthermore, the expression should be independent of stimuli such as cytokines or ROS and of cell cycles. Finally, it is best that the characteristics of the transfectant do not differ from those of the parent cell line. Before *in vivo* studies, we examined the characteristics of the transfectant, B16-BL6/Luc cells. The luciferase activity of the cells was stable for at least 1 year and proportional to the cell number over a wide range. The expression of the luciferase in the cells was hardly affected by the growth phase, the addition of H₂O₂, or catalase. These properties are consistent with previous results showing that for plasmid DNA encoding *firefly luciferase* under the control of cytomegalovirus, immediate early promoter activity was independent of the cell cycle (21), and the expression level was scarcely affected after inoculation into mice (22). In addition, the half-life of firefly luciferase is very short (about 3 hours); therefore, the level of the luciferase protein in the cell would level off quickly. These properties enable us to use the luciferase activity in lung tissue as an indicator of the exact number of tumor cells.

In the experimental pulmonary metastasis model, B16-BL6 or B16-BL6/Luc melanoma cells were injected intravenously into syngeneic C57BL/6 mice. Therefore, the first step in the pulmonary metastasis is the arrest of the tumor cells in small vessels in the lung followed by their adhesion to endothelial cells (1, 23). As shown in Fig. 2, intravenous injection of B16-BL6/Luc cells resulted in the accumulation of 60 to 90% of the injected cells in the lung and few in other organs at 1 hour after tumor injection. Thereafter, the tumor cells in the lung fell to 2 to 4% of the injected cells at 24 hours. In contrast, when injected into the portal vein, about 60% of the injected B16-BL6/Luc cells were detected even at 24 hours after injection.³ These results of organ- or cell number-independent tumor cell arrest suggest that the initial step in the formation of metastatic colonies of B16 tumor cells is mediated by physical trapping of the cells within the microvasculature of organs rather than by a specific interaction between tumor cells and endothelial cells via adhesion molecules. The tumor cells arrested in the lung could be destroyed in the microvasculature by mechanical stress caused by respiration in the first 24 hours after tumor injection. Because the injected tumor cells decreased to 2–4% irrespective of the initial number of cells, this inefficiency could be because of the physical forces of contraction and relaxation of the lung tissue but not to immunity. It is also suggested that at 24 hours

³ Unpublished data.

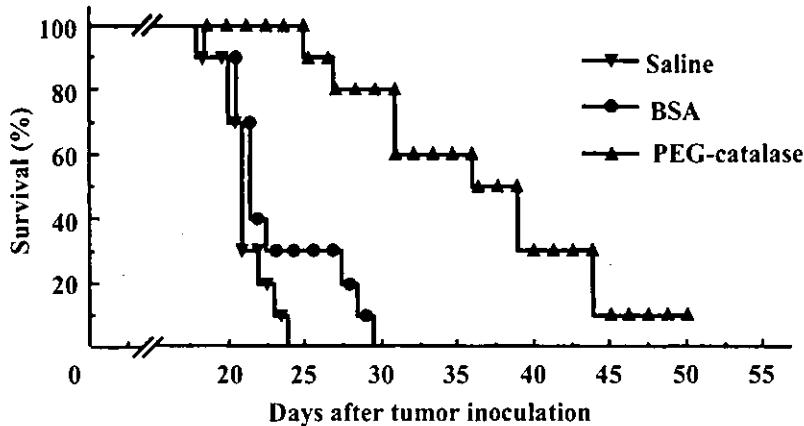


Fig. 6 Survival of mice receiving intravenous injection of B16-BL6 cells (1×10^4 cells/mouse). Saline (vehicle), PEG-catalase or BSA was injected daily into the tail vein until 30 days after tumor inoculation. The survival of the PEG-catalase treatment group was significantly longer than that of the saline ($P < 0.0001$) or BSA ($P < 0.01$) treatment group ($n = 10$).

after tumor injection, the injected tumor cells adhere completely to the endothelium and the surviving tumor cells are ready to extravasate and invade the parenchyma of the lung. From day 1 to 3, the tumor cells could have invaded the parenchyma and started to proliferate. An intravital videomicroscopic analysis supports this hypothesis (24).

Even under normal conditions, ROS are continuously produced as by-products of metabolism by enzymes such as superoxide dismutase, xanthine oxidase, and NADPH oxidase (25). Several antitumor drugs as well as radiation also generate ROS through reductive activation and redox recycling (25–27), and it has also been reported that ROS are involved in various processes of tumor metastasis, such as adhesion, invasion and proliferation (5, 6, 9–12). Therefore, the scavenging of ROS by antioxidant enzymes can be an effective approach for inhibiting tumor metastasis. We have proposed a hypothesis that the elimination of H_2O_2 at the site where tumor metastasis occurs reduces this and we have examined the effect of increasing the plasma half-life of catalase on the inhibition of an experimental pulmonary metastasis (8). We found that intravenous injection of PEG-catalase greatly decreased the number of colonies in the lung 2 weeks after tumor injection and, in a separate set of experiments, we have shown that targeted delivery of catalase to hepatocytes greatly inhibited experimental hepatic metastasis in mice (28). These results indicate that the detoxification of H_2O_2 is a promising approach for inhibiting metastasis. However, these results did not identify which metastatic processes are inhibited by the catalase derivatives. To address this question, we measured the number of tumor cells in the lung at 1 hour, 1 and 7 days after injection of tumor cells and examined the effects of catalase derivatives on the metastatic processes.

Administration of PEG-catalase just before tumor injection, which is the same protocol as the one used in a previous study (8), reduced the number of tumor cells in the lung at 24 hours after tumor injection, indicating that PEG-catalase inhibits the early steps of metastasis. Additional studies are needed to identify whether changes in the expression of adhesion molecules are involved in the inhibitory effect of catalase derivatives in the lung. PEG-catalase was effective in reducing the number of tumor cells at day 7, even when intravenously injected at 1 or 3 days after tumor injection. As shown in Fig. 2, the tumor cells

in the lung were in a growth phase at the times when PEG-catalase was injected. Therefore, these results indicate that scavenging of H_2O_2 by PEG-catalase can inhibit the growth of metastatic tumor cells. It has already been reported that H_2O_2 can accelerate proliferation (12); therefore, the suppressive effect of catalase derivatives would be attributable to direct inhibition of the proliferation of tumor cells. As shown in Fig. 5B, a single injection of PEG-catalase just before tumor injection reduced the number of metastatic nodules but scarcely affected the diameter of the nodules. After triple injection of PEG-catalase (just before, 1 and 3 days after tumor injection), the number of metastatic colonies did not markedly differ from that produced by a single (just before tumor injection) or double (just before and 1 day after tumor injection) injection, although the diameter of the colonies was found to be small. These findings indicate that the first injection of PEG-catalase reduces the number of surviving tumor cells, and the subsequent injections inhibit the proliferation of the surviving tumor cells. Therefore, it is suggested that PEG-catalase inhibits not only the survival or adhesion of tumor cells but also their invasion and proliferation.

Thus, it has been shown that catalase derivatives effectively inhibit not only the early steps of metastasis, but also the later steps. Then, we tried to effectively suppress metastatic tumor growth by inducing tumor dormancy. As shown in Fig. 5A, daily injection of PEG-catalase greatly reduced the number of tumor cells detected at 14 days in the lung. The number of tumor cells scarcely increased compared with that detected at 24 hours after tumor injection. Therefore, the tumor cells within the lung tissue may be in a dormant state after repetitive injection of PEG-catalase. This significant inhibition of growth was effective in increasing the survival of the tumor-bearing mice. However, the mice treated with PEG-catalase died sequentially after stopping the injection, suggesting that the tumor cells of micro-metastases start to proliferate when the supply of catalase is stopped. In previous publications (29, 30), “dormancy” was used to refer to individual tumor cells that were thought to persist “symbiotically” for long periods, but subsequently could be stimulated to exhibit malignant growth. Therefore, the results of the present study indicate that repeated administration of PEG-catalase can induce tumor dormancy and prolong the survival period.

In conclusion, we have developed a quantitative method to analyze tissue disposition of tumor cells and found that scavenging of H₂O₂ by PEG-catalase can effectively inhibit not only the early steps of metastasis, such as embolization, adhesion, or survival, but also later steps, such as invasion or proliferation. Continuous supply of catalase activity within the blood circulation by multiple dosing of PEG-catalase greatly suppressed the growth of tumor cells in metastatic foci. This reduction of metastatic tumor growth by PEG-catalase offers potentially a very effective approach to the antimetastatic therapy of a variety of tumors.

REFERENCES

- Engers R, Gabbert HE. Mechanisms of tumor metastasis: cell biological aspects and clinical implications. *J Cancer Res Clin Oncol* 2000;126:682-92.
- Zetter BR. The cellular basis of site-specific tumor metastasis. *N Engl J Med* 1990;322:605-12.
- Tang DG, Honn KV. Adhesion molecules and tumor metastasis: an update. *Invasion Metastasis* 14:109-22, 1994.
- Kannagi R. Carbohydrate-mediated cell adhesion involved in hemogenous metastasis of cancer. *Glycoconj J* 1997;14:577-84.
- Onoda JM, Piechocki MP, Honn KV. Radiation-induced increase in expression of the alpha IIb beta 3 integrin in melanoma cells: effects on metastatic potential. *Radiat Res* 1992;130:281-8.
- Sellak H, Franzini E, Hakim J, Pasquier C. Reactive oxygen species rapidly increase endothelial ICAM-1 ability to bind neutrophils without detectable upregulation. *Blood* 1994;83:2669-77.
- Willam C, Schindler R, Frei U, Eckardt KU. Increases in oxygen tension stimulate expression of ICAM-1 and VCAM-1 on human endothelial cells. *Am J Physiol* 1999;276:H2044-52.
- Nishikawa M, Tamada A, Kumai H, Yamashita F, Hashida M. Inhibition of experimental pulmonary metastasis by controlling biodistribution of catalase in mice. *Int J Cancer* 2002;99:474-9.
- Shaughnessy SG, Whaley M, Lafrenie RM, Orr FW. Walker 256 tumor cell degradation of extracellular matrices involves a latent gelatinase activated by reactive oxygen species. *Arch Biochem Biophys* 1993;304:314-21.
- Rajagopalan S, Meng XP, Ramasamy S, Harrison DG, Galis ZS. Reactive oxygen species produced by macrophage-derived foam cells regulate the activity of vascular matrix metalloproteinases in vitro. Implications for atherosclerotic plaque stability. *J Clin Invest* 1996;98:2572-9.
- Belkhiri A, Richards C, Whaley M, McQueen SA, Orr FW. Increased expression of activated matrix metalloproteinase-2 by human endothelial cells after sublethal H₂O₂ exposure. *Lab Invest* 1997;77:533-9.
- Murrell GA, Francis MJ, Bromley L. Modulation of fibroblast proliferation by oxygen free radicals. *Biochem J* 1990;265:659-65.
- Zhang L, Hellstrom KE, Chen L. Luciferase activity as a marker of tumor burden and as an indicator of tumor response to antineoplastic therapy in vivo. *Clin Exp Metastasis* 1994;12:87-92.
- El Hilali N, Rubio N, Martinez-Villacampa M, Blanco J. Combined noninvasive imaging and luminometric quantification of luciferase-labeled human prostate tumors and metastases. *Lab Invest* 2002;82:1563-71.
- Edinger M, Sweeney TJ, Tucker AA, Olomu AB, Negrin RS, Contag CH. Noninvasive assessment of tumor cell proliferation in animal models. *Neoplasia* 1999;1:303-10.
- Vooijs M, Jonkers J, Lyons S, Berns A. Noninvasive imaging of spontaneous retinoblastoma pathway-dependent tumors in mice. *Cancer Res* 2002;62:1862-7.
- Ray P, Wu AM, Gambhir SS. Optical bioluminescence and positron emission tomography imaging of a novel fusion reporter gene in tumor xenografts of living mice. *Cancer Res* 2003;63:1160-5.
- Yabe Y, Nishikawa M, Tamada A, Takakura Y, Hashida M. Targeted delivery and improved therapeutic potential of catalase by chemical modification: combination with superoxide dismutase derivatives. *J Pharmacol Exp Ther* 1999;289:1176-84.
- Poste G, Doll J, Hart IR, Fidler IJ. In vitro selection of murine B16 melanoma variants with enhanced tissue-invasive properties. *Cancer Res* 1980;40:1636-44.
- Nishikawa M, Yamauchi M, Morimoto K, Ishida E, Takakura Y, Hashida M. Hepatocyte-targeted in vivo gene expression by intravenous injection of plasmid DNA complexed with synthetic multi-functional gene delivery system. *Gene Ther* 2000;7:548-55.
- Honda M, Kaneko S, Matsushita E, Kobayashi K, Abell GA, Lemon SM. Cell cycle regulation of hepatitis C virus internal ribosomal entry site-directed translation. *Gastroenterology* 2000;118:152-62.
- Rubio N, Espana L, Fernandez Y, Blanco J, Sierra A. Metastatic behavior of human breast carcinomas overexpressing the Bcl-x(L) gene: a role in dormancy and organospecificity. *Lab Invest* 2001;81:725-34.
- Blood CH, Zetter BR. Tumor interactions with the vasculature: angiogenesis and tumor metastasis. *Biochim Biophys Acta* 1990;1032:89-118.
- Luzzi KJ, MacDonald IC, Schmidt EE, et al. Multistep nature of metastatic inefficiency: dormancy of solitary cells after successful extravasation and limited survival of early micrometastases. *Am J Pathol* 1998;153:865-73.
- Warner HR. Superoxide dismutase, aging, and degenerative disease. *Free Radic Biol Med* 1994;17:249-58.
- Maliszka KL, McIntosh AR, Sveinson SE, Hasinoff BB. Semiquinone free radical formation by daunorubicin aglycone incorporated into the cellular membranes of intact Chinese hamster ovary cells. *Free Radic Res* 1996;24:9-18.
- Lazo JS, Sebt SM, Schellens JH. Bleomycin. *Cancer Chemother Biol Response Modif* 1996;16:39-47.
- Nishikawa M, Tamada A, Hyoudou K, et al. Inhibition of experimental hepatic metastasis by targeted delivery of catalase in mice. *Clin Exp Metastasis*. 2004;21:213-21.
- Hadfield G. The dormant cancer cell. *Br Med J* 1954;4888:607-10.
- Fisher B, Fisher ER. Experimental evidence in support of the dormant tumor cell. *Science (Wash D C)* 1959;130:918-9.



Inhibition of experimental hepatic metastasis by targeted delivery of catalase in mice

Makiya Nishikawa¹, Ayumi Tamada¹, Kenji Hyoudou¹, Yukari Umeyama¹, Yuki Takahashi², Yuki Kobayashi¹, Hitomi Kumai¹, Emi Ishida¹, Frantisek Staud¹, Yoshiyuki Yabe¹, Yoshinobu Takakura², Fumiyoshi Yamashita¹ & Mitsuru Hashida¹

Departments of ¹Drug Delivery Research, and ²Biopharmaceutics and Drug Metabolism, Graduate School of Pharmaceutical Sciences, Kyoto University, Sakyo-ku, Kyoto, Japan

Received 25 July 2003; accepted in revised form 25 March 2004

Key words: asialoglycoprotein receptor, catalase, matrix metalloproteinase, metastasis, reactive oxygen species

Abstract

Bovine liver catalase derivatives possessing diverse tissue distribution properties were synthesized, and their effects on hepatic metastasis of colon carcinoma cells were examined in mice. An intraportal injection of 1×10^5 colon 26 cells resulted in the formation of more than 50 metastatic colonies on the surface of the liver at 14 days after injection. An intravenous injection of catalase (CAT; 35 000 units/kg of body weight) significantly ($P < 0.001$) reduced the number of the colonies in the liver. Galactosylated (Gal-), mannosylated (Man-) and succinylated (Suc-) CAT were also tested in the same system. Of these derivatives, Gal-CAT showed the greatest inhibitory effect on hepatic metastasis, and the number of colonies was significantly ($P < 0.001$) smaller than following treatment with catalase. High activities of matrix metalloproteinases (MMPs), especially MMP-9, were detected in the liver of mice bearing metastatic tumor tissues, which was significantly ($P < 0.05$) reduced by Gal-CAT. These results, combined with our previous finding that Gal-CAT can be efficiently delivered to hepatocytes, indicate that the targeted delivery of catalase to the liver by galactosylation is a promising approach to suppress hepatic metastasis. Decreased MMP activity by catalase delivery seems to be involved in its anti-metastatic effect.

Abbreviations: CAT – bovine liver catalase; ECM – extracellular matrix; Gal – galactosylated; HBSS – Hanks' balanced salt solution; H_2O_2 – hydrogen peroxide; Man – mannosylated; MMP – matrix metalloproteinase; ROS – reactive oxygen species; Suc – succinylated; SOD – superoxide dismutase

Introduction

Metastasis is the most characteristic aspect of malignant neoplasms and is the leading cause of death in cancer patients. Tumor metastasis involves: tumor cell dissociation, invasion, intravasation, distribution to distant organs, arrest in small vessels, adhesion to endothelial cells, extravasation, invasion of the target organ, and proliferation [1], as well as angiogenesis at the original and target sites. Reactive oxygen species (ROS) regulate the expression levels of molecules involved in the above metastatic processes. Expression levels of adhesion molecules are regulated by several factors including ROS [2, 3]. Matrix metalloproteinases (MMPs) and other proteases, produced by either tumor cells or non-tumor cells, are important for proteolytic degradation of extracellular matrix (ECM) and basement membranes, whose expression or activation is, at least partially, controlled by

the presence of ROS [4–6]. In an actual fact, ROS increase the invasive activity of tumor cells beneath a cultured mesothelial monolayer [7]. In addition, low level ROS, especially hydrogen peroxide (H_2O_2), are known to increase *in vitro* proliferation of cell [8]. ROS-mediated injuries to endothelial cells facilitate the local arrest of circulating tumor cells and the subsequent growth of metastatic tumors at the site [9]. Large amounts of H_2O_2 are produced and excreted by human tumor cells [10] and this might be used as a means of enhancing tumor invasion and proliferation.

On the other hand, ROS generated from antitumor drugs are known to exhibit antitumor effects due to their highly cytotoxic nature. Therefore, ROS-generating enzyme systems have been examined as a possible approach for antitumor treatment [11, 12]. Jessup et al. [13] showed that ROS generated by the resumption of blood flow that had been stopped due to the embolization of tumor cells could kill metastatic precursor cells. These findings, together with the results showing ROS-mediated increase in the expression of factors enhancing tumor metastasis, severely complicate the effects of ROS on tumor metastasis. Furthermore, there

Correspondence to: Makiya Nishikawa, PhD, Department of Drug Delivery Research, Graduate School of Pharmaceutical Sciences, Kyoto University, Sakyo-ku, Kyoto 606-8501, Japan. Tel: +81-75-7534616; Fax: +81-75-7534614; E-mail: makiya@pharm.kyoto-u.ac.jp